Finite element approximation of transmission conditions in fluids and solids introducing boundary subgrid scales

Ramon Codina*,† and Joan Baiges

Universitat Politècnica de Catalunya, Jordi Girona 1-3, Edifici C1, 08034 Barcelona, Spain

SUMMARY

Terms involving jumps of stresses on boundaries are proposed for the finite element approximation of the Stokes problem and the linear elasticity equations. These terms are designed to improve the transmission conditions between subdomains at three different levels, namely, between the element domains, between the interfaces in homogeneous domain interaction problems and at the interface between the fluid and the solid in fluid–structure interaction problems. The benefits in each case are respectively the possibility of using discontinuous pressure interpolations in a stabilized finite element approximation of the Stokes problem, a stronger enforcement of the stress continuity in homogeneous domain decomposition problems and a considerable improvement of the behavior of iterative schemes to couple the fluid and the solid in fluid–structure integration algorithms. The motivation to introduce these terms stems from a decomposition of the unknown into a conforming and a non-conforming part, a hybrid formulation for the latter and a simple approximation for the unknowns involved in the hybrid problem. Copyright © 2011 John Wiley & Sons, Ltd.

A paper dedicated to the memory of Professor O.C. Zienkiewicz. The first author wishes to acknowledge the unique opportunity he had of collaborating with a person like him, and to witness his passion and his creativity, even in the latest stages of his long and fruitful scientific career

1. INTRODUCTION

Transmission conditions in the numerical approximation of fluid and solid mechanics problems play a key role at different levels. When the discretization involves a partition of the computational domain, as in finite volume or finite element methods, the first level is the interaction between the subdomains of the partition. Appropriate interaction conditions, associated with the problem being solved, are satisfied in an approximate way, and this may have important consequences in the stability of the numerical method. A second level of analysis of transmission conditions could be the interaction of subdomains in a homogeneous domain decomposition method. This problem may be addressed using a purely algebraic point of view, but it is also possible to analyze the interaction from the standpoint of the approximate boundary conditions applied to each subdomain. Both strategies are well known in the domain decomposition community (see [1, 2], for example).

---

*Correspondence to: Ramon Codina, Universitat Politècnica de Catalunya, Jordi Girona 1-3, Edifici C1, 08034 Barcelona, Spain.
†E-mail: ramon.codina@upc.edu

A third level of analysis could be the interaction between *heterogeneous* subdomains, in which different problems associated with different physics are solved within each of the subdomains. This last category could be included in the second, but the heterogeneity of the transmission conditions introduces additional difficulties that deserve to be studied independently. The paradigmatic example of this class of problems are those involving fluid and structure interactions (FSIs).

In this work, we analyze the issue of dealing with transmission conditions in fluid and solid mechanics problems approximated using finite elements. The model problems we will consider are the Stokes problem and the Navier equations for a linear elastic solid. Our proposal is to modify the classical approximation of the interaction stresses computed from the finite element solution by introducing terms that depend on the jumps of these stresses when computed from the two sides of the interaction boundary. The way to motivate the introduction of these terms is as follows. First, we consider a splitting of the unknown into a conforming and a discontinuous part. A three-field hybrid formulation is used for the latter, involving the primal variable, its traces and its fluxes on the element boundaries as unknowns. We assume that these terms are *small*, and therefore we consider them as *subgrid scales* (or subscales) of the conforming part of the solution. In this sense, our approach falls within the variational multiscale framework proposed in [3]. Rather than solving for the subscales, we propose simple expressions to *model* them, the main idea being the correct continuity of stresses across the interelement boundaries.

When solving for the Stokes problem in a single domain, the introduction of the element boundary terms involving jumps of stresses has as a consequence a stabilizing effect on the pressure. In particular, in combination with a more standard stabilized finite element method, these new terms open the possibility to use arbitrary discontinuous pressure interpolations, avoiding the need to satisfy the classical velocity–pressure compatibility conditions [4]. Their stabilizing effect is similar to that already found in [5], although their expression is different and motivated in a completely different way.

Pressure stabilization due to the new interelement boundary terms was already proposed and analyzed in [6]. In the present work, we derive in detail the formulation for the Stokes problem (which in the reference mentioned was directly stated from the derivation obtained for the convection–diffusion equation), with emphasis on the treatment of Neumann boundary conditions. This serves us to extend it to two cases, namely, the interaction between two subdomains, in each of which the Stokes problem is solved, and the classical FSI problem. In the first case, the new terms we propose help to enforce the continuity of stresses between subdomains. The domain interaction is however more complex than in classical formulations. To introduce an iteration-by-subdomain scheme, we first analyze the matrix structure of the problem and discuss how this iterative scheme can be designed. In the FSI case, we apply the previous ideas to a time-marching block-iterative scheme in which Dirichlet boundary conditions are prescribed to the fluid and Neumann boundary conditions are applied to the solid. The latter correspond to the normal stress exerted by the fluid on the solid. The introduction of the subscales on the element boundaries for the solid enhances notably the stability of the scheme. We illustrate this enhancement with a numerical example. In particular, the example we have chosen displays the so-called added-mass effect, which is one of the most important issues to be considered when solving FSI problems by means of a domain decomposition technique. This phenomenon takes place when fluid and solid densities are similar, and consists of a failing of simple coupling strategies (this is the sense in which the term 'added-mass effect' is used in this paper). Whether if the coupling is implicit (iterating the solution at each time step to converge to the monolithic problem) or explicit (no coupling iterations are done within the time step), the scheme becomes unstable. Several strategies to deal with this problem have been recently proposed. For example, a semi-implicit scheme for pressure-segregated methods is presented in [7], and is further developed in [8]. A different approach for pressure-segregated schemes is proposed in [9]. In [10], a strategy based on Nitsche's method is proposed and a method based on Robin boundary conditions can be found in [11]. Using a more algebraic point of view, several strategies using preconditioned Krylov methods are presented in [12–14]. Conditions under which the problem becomes unstable are studied in [15]. We present here our own approach, which is directly derived from the use of boundary subgrid scales.

The paper is organized as follows. In Section 2 we state the Stokes problem in strong form, in the classical velocity–pressure variational form and in a non-standard hybrid variational form that we use to motivate our numerical formulation. This formulation is presented in detail in Section 3. The final result is a problem posed only for a conforming approximation to the velocity and the pressure that involves jumps of stresses at the interelement boundaries. The application of the same ideas to a homogeneous domain interaction problem is presented in Section 4, whereas the application to the FSI problem is the subject of Section 5. Numerical examples are presented in Section 6 and finally conclusions close the paper in Section 7.

2. PROBLEM STATEMENT

2.1. Stokes problem in $\boldsymbol{u}$-p form

Let us start by considering the Stokes problem written in the classical velocity–pressure approach or displacement–pressure, in the case of an elastic solid. To fix the terminology, we will consider that it corresponds to a fluid, leaving for Section 5 the statement of the elastic problem. Thus, the problem we consider here consists of finding a velocity $\boldsymbol{u}:\Omega \longrightarrow \mathbb{R}^d$ and a pressure $p:\Omega \longrightarrow \mathbb{R}$ such that

$$-\mu \Delta \boldsymbol{u} + \nabla p = \rho \boldsymbol{f} \quad \text{in } \Omega, \tag{1}$$

$$\nabla \cdot \boldsymbol{u} = 0 \quad \text{in } \Omega, \tag{2}$$

$$\boldsymbol{u} = \boldsymbol{0} \quad \text{on } \Gamma_{\mathrm{D}}, \tag{3}$$

$$-p\boldsymbol{n} + \mu \boldsymbol{n} \cdot \nabla \boldsymbol{u} = \boldsymbol{t} \quad \text{on } \Gamma_{\mathrm{N}}. \tag{4}$$

In these equations, $\Omega \subset \mathbb{R}^d$ ($d = 2, 3$) is a bounded domain with boundary $\partial \Omega$ and external normal $\boldsymbol{n}$, $\boldsymbol{f}$ is the vector of body forces and $\boldsymbol{t}$ is the (pseudo-)traction prescribed on Γ_{N}, with $\partial \Omega = \overline{\Gamma_{\mathrm{N}} \cup \Gamma_{\mathrm{D}}}$, $\Gamma_{\mathrm{N}} \cap \Gamma_{\mathrm{D}} = \emptyset$, $\Gamma_{\mathrm{D}} \neq \emptyset$. The physical parameters μ and ρ are the viscosity and the density, respectively. Note that the Neumann-type conditions do not correspond to the physically meaningful tractions, for which the viscous term should be written using the symmetrical gradient of the velocity. This, however, is irrelevant for our discussion.

Let now $V = H_{\Gamma}^1(\Omega)^d := \{\boldsymbol{v} \in H^1(\Omega)^d | \boldsymbol{v} = \boldsymbol{0} \text{ on } \Gamma_{\mathrm{D}}\}$, $Q = L^2(\Omega)$, and assume that $\boldsymbol{f} \in (H_{\Gamma}^1(\Omega)^d)'$ (the dual space of $H_{\Gamma}^1(\Omega)^d$) and $\boldsymbol{t} \in H^{-1/2}(\Gamma_{\mathrm{N}})^d$. We will use the symbol $(\cdot, \cdot)_\omega$ to denote the L^2 product in a domain ω. In general, the integral of two functions g_1 and g_2 over a domain ω will be denoted by $\langle g_1, g_2 \rangle_\omega$. This symbol will also be used for the duality pairing. The simplifications $(\cdot, \cdot)_\Omega \equiv (\cdot, \cdot)$ and $\langle \cdot, \cdot \rangle_\Omega \equiv \langle \cdot, \cdot \rangle$ will be used.

The variational problem consists of finding $[\boldsymbol{u}, p] \in V \times Q$ such that

$$B([\boldsymbol{u}, p], [\boldsymbol{v}, q]) = L([\boldsymbol{v}, q]) + \langle \boldsymbol{t}, \boldsymbol{v} \rangle_{\Gamma_{\mathrm{N}}} \quad \forall [\boldsymbol{v}, q] \in V \times Q,$$

where

$$B([\boldsymbol{u}, p], [\boldsymbol{v}, q]) := \mu(\nabla \boldsymbol{u}, \nabla \boldsymbol{v}) - (p, \nabla \cdot \boldsymbol{v}) + (q, \nabla \cdot \boldsymbol{u}),$$

$$L([\boldsymbol{v}, q]) := \rho \langle \boldsymbol{f}, \boldsymbol{v} \rangle.$$

2.2. Hybrid formulation of an abstract variational problem

The numerical approximation we propose can be motivated from a hybrid formulation of the problem. To introduce it, let us assume that $\bar{\Omega} = \bar{\Omega}_1 \cup \bar{\Omega}_2$, with $\Gamma = \partial \Omega_1 \cap \partial \Omega_2$ (see Figure 1).

Consider an abstract variational problem consisting of finding an unknown u in a functional space X such that

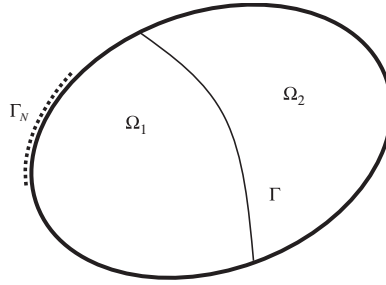$$a(u, v) = l(v) \quad \forall v \in X, \tag{5}$$

Figure 1. Splitting of the domain.

where $a(u, v)$ is a bilinear form on $X \times X$ and l a linear form defined on X. Let u_i, v_i be the restrictions of $u, v \in X$ to subdomain Ω_i, and X_i the spaces where they belong, $i = 1, 2$. Suppose that $u \in X$ has a well-defined trace on Γ belonging to a space T, and a flux corresponding to the differential operator associated with (5) belonging to a space F_i when computed from subdomain Ω_i, $i = 1, 2$. Then, the hybrid formulation of (5) that we consider is the following: find $u_i \in X_i$, $\lambda_i \in F_i$, $i = 1, 2$, and $\gamma \in T$ such that

$$a_1(u_1, v_1) - \langle \lambda_1, v_1 \rangle_\Gamma = l_1(v_1) \quad \forall v_1 \in X_1,$$

$$a_2(u_2, v_2) - \langle \lambda_2, v_2 \rangle_\Gamma = l_2(v_2) \quad \forall v_2 \in X_2,$$

$$\langle \mu_1, u_1 - \gamma \rangle_\Gamma = 0 \quad \forall \mu_1 \in F_1,$$

$$\langle \mu_2, u_2 - \gamma \rangle_\Gamma = 0 \quad \forall \mu_2 \in F_2,$$

$$\langle \kappa, \lambda_1 + \lambda_2 \rangle_\Gamma = 0 \quad \forall \kappa \in T,$$

where a_i and l_i are the restrictions of a and l to $X_i \times X_i$ and X_i, respectively.

If the problem includes imposition of fluxes of u in a part Γ_N of $\partial\Omega$, which for the sake of simplicity we may consider contained in $\partial\Omega_1$ (see Figure 1), this imposition may be also 'hybridized', yielding the problem

$$a_1(u_1, v_1) - \langle \lambda_1, v_1 \rangle_\Gamma - \langle \lambda_N, v_1 \rangle_{\Gamma_N} = l_1(v_1) \quad \forall v_1 \in X_1, \tag{6}$$

$$a_2(u_2, v_2) - \langle \lambda_2, v_2 \rangle_\Gamma = l_2(v_2) \quad \forall v_2 \in X_2, \tag{7}$$

$$\langle \mu_1, u_1 - \gamma \rangle_\Gamma + \langle \mu_1, u_1 - \gamma \rangle_{\Gamma_N} = 0 \quad \forall \mu_1 \in F_1, \tag{8}$$

$$\langle \mu_2, u_2 - \gamma \rangle_\Gamma = 0 \quad \forall \mu_2 \in F_2, \tag{9}$$

$$\langle \kappa, \lambda_1 + \lambda_2 \rangle_\Gamma + \langle \kappa, \lambda_N \rangle_{\Gamma_N} = \langle \kappa, q \rangle_{\Gamma_N} \quad \forall \kappa \in T, \tag{10}$$

where q is the flux to be prescribed. In this case, the linear form l (and the forms l_1 and l_2 resulting from the splitting of the domain) does *not* include the prescription of the fluxes.

Several problems admit this hybrid formulation, including first- and second-order linear partial differential equations (the fluxes λ_i are zero in the first case). In the following subsection, we shall see its application to the Stokes problem. For the diffusion equation $-\Delta u = f$ with $u = 0$ on $\partial\Omega$, we would have that X_i is the subspace of $H^1(\Omega_i)$ of functions vanishing on $\partial\Omega \cap \partial\Omega_i$, $T = H_{00}^{1/2}(\Gamma)$ and $F_i = (H_{00}^{1/2}(\Gamma_i))'$ (the prime denoting dual space), with $\Gamma_i = \partial\Omega_i \cap \Omega$. The solution of the hybrid problem is $\gamma = u_1|_{\Gamma_1} = u_2|_{\Gamma_2}$, $\lambda_1 = -\lambda_2 = \boldsymbol{n}_1 \cdot \nabla u_1|_{\Gamma_1} = -\boldsymbol{n}_2 \cdot \nabla u_2|_{\Gamma_2}$. If flux conditions need to be prescribed, in this case they are of the form $\boldsymbol{n} \cdot \nabla u = q$, and Γ_1 will contain Γ_N, the part of the boundary where these conditions are enforced.

2.3. Hybrid formulation of the Stokes problem

The Stokes problem (1)–(2) admits also the hybrid formulation described above by defining

$$u = [\boldsymbol{u}, p], \quad v = [\boldsymbol{v}, q], \quad X = V \times Q,$$

$$a(u, v) = B([\boldsymbol{u}, p], [\boldsymbol{v}, q]), \quad l(v) = L([\boldsymbol{v}, q]),$$

$$\gamma = \boldsymbol{u}_1|_{\Gamma_1} = \boldsymbol{u}_2|_{\Gamma_2} \in T = H_{00}^{1/2}(\Gamma)^d,$$

$$\lambda_i = (-p\boldsymbol{n}_i + \mu\boldsymbol{n}_i \cdot \nabla \boldsymbol{u})|_{\Gamma_i} \in F_i = (H_{00}^{1/2}(\Gamma_i)^d)', \quad i = 1, 2,$$

and $q = \boldsymbol{t}$ (see (4)) being the boundary condition in terms of fluxes.

To present the formulation we are interested in, let us consider a splitting of space V of the form $V = \bar{V} \oplus \tilde{V}$. In principle, there is no restriction in the expression of spaces $\bar{V}$ and $\tilde{V}$. In the finite element approximation, the former will be approximated by *continuous* finite elements (and therefore conforming). The component of $\boldsymbol{u}$ in this space can be considered as *resolvable*, whereas a closed-form expression will be given for the component in $\tilde{V}$, which will be called *subgrid scale* or, simply, *subscale*. A similar splitting could be performed for the pressure, although it is not necessary for our purposes.

Let V_i be also split as $V_i = \bar{V}_i \oplus \tilde{V}_i$, $i = 1, 2$. If any $\boldsymbol{u}_i \in V_i$ is written as $\boldsymbol{u}_i = \bar{\boldsymbol{u}}_i + \tilde{\boldsymbol{u}}_i$, with $\bar{\boldsymbol{u}}_i \in \bar{V}_i$ and $\tilde{\boldsymbol{u}}_i \in \tilde{V}_i$, we assume that $\bar{\boldsymbol{u}}_1|_{\Gamma_1} = \bar{\boldsymbol{u}}_2|_{\Gamma_2}$. Only the continuity for the component in $\tilde{V}_i$ needs to be enforced (weakly) through a variational equation.

Let us introduce the boundary operators

$$\mathscr{T}_i([\bar{\boldsymbol{v}}_i, q_i]) := (-q_i\boldsymbol{n}_i + \mu_i\boldsymbol{n}_i \cdot \nabla \bar{\boldsymbol{v}}_i)|_{\Gamma_i}, \quad \mathscr{T}_i^*([\bar{\boldsymbol{v}}_i, q_i]) := (q_i\boldsymbol{n}_i + \mu_i\boldsymbol{n}_i \cdot \nabla \bar{\boldsymbol{v}}_i)|_{\Gamma_i},$$

where $[\boldsymbol{v}_i, q_i] \in \bar{V}_i \times Q_i$, $i = 1, 2$. We may constrain the fluxes to be of the form $\lambda_i = \mathscr{T}_i([\bar{\boldsymbol{u}}_i, p_i]) + \tilde{\lambda}_i$, for appropriate $\tilde{\lambda}_i \in \tilde{F}_i$, and likewise for λ_N. Test functions in F_i can be similarly split as $\mu_i = \mathscr{T}_i^*([\bar{\boldsymbol{v}}_i, q_i]) + \tilde{\mu}_i$, with $\bar{\boldsymbol{v}}_i \in \bar{V}_i$, $q_i \in Q_i$, $\tilde{\mu}_i \in \tilde{F}_i$. Finally, traces on boundaries can be split as $\gamma = \bar{\boldsymbol{u}} + \tilde{\gamma}$, both on Γ and on Γ_N. On the intersecting boundary Γ, the restriction $\bar{\boldsymbol{u}}$ is well defined because of the assumption $\bar{\boldsymbol{u}}_1|_{\Gamma_1} = \bar{\boldsymbol{u}}_2|_{\Gamma_2}$. Note that, in fact, $\tilde{F}_i = F_i$ and $\tilde{T} = T$. The tilde has been introduced to stress that we seek the subscale of fluxes and traces in these spaces.

Having introduced these decompositions of the functional spaces, we may write the hybrid formulation of the Stokes problem as follows: find $\bar{\boldsymbol{u}}_i \in \bar{V}_i$, $\tilde{\boldsymbol{u}}_i \in \tilde{V}_i$, $p_i \in Q_i$, $\tilde{\gamma} \in \tilde{T}$, $\tilde{\lambda}_i \in \tilde{F}_i$ ($i = 1, 2$) such that

$$B_1([\bar{\boldsymbol{u}}_1 + \tilde{\boldsymbol{u}}_1, p_1], [\bar{\boldsymbol{v}}_1 + \tilde{\boldsymbol{v}}_1, q_1]) - \langle \mathscr{T}_1([\bar{\boldsymbol{u}}_1, p_1]) + \tilde{\lambda}_1, \bar{\boldsymbol{v}}_1 + \tilde{\boldsymbol{v}}_1 \rangle_\Gamma$$
$$- \langle \mathscr{T}_1([\bar{\boldsymbol{u}}_1, p_1]) + \tilde{\lambda}_N, \bar{\boldsymbol{v}}_1 + \tilde{\boldsymbol{v}}_1 \rangle_{\Gamma_N} = L_1([\bar{\boldsymbol{v}}_1 + \tilde{\boldsymbol{v}}_1, q_1]), \tag{11}$$

$$B_2([\bar{\boldsymbol{u}}_2 + \tilde{\boldsymbol{u}}_2, p_2], [\bar{\boldsymbol{v}}_2 + \tilde{\boldsymbol{v}}_2, q_2]) - \langle \mathscr{T}_2([\bar{\boldsymbol{u}}_2, p_2]) + \tilde{\lambda}_2, \bar{\boldsymbol{v}}_2 + \tilde{\boldsymbol{v}}_2 \rangle_\Gamma = L_2([\bar{\boldsymbol{v}}_2 + \tilde{\boldsymbol{v}}_2, q_2]), \tag{12}$$

$$\langle \mathscr{T}_1^*([\bar{\boldsymbol{v}}_1, q_1]) + \tilde{\mu}_1, \tilde{\gamma} - \tilde{\boldsymbol{u}}_1 \rangle_\Gamma + \langle \mathscr{T}_1^*([\bar{\boldsymbol{v}}_1, q_1]) + \tilde{\mu}_1, \tilde{\gamma} - \tilde{\boldsymbol{u}}_1 \rangle_{\Gamma_N} = 0, \tag{13}$$

$$\langle \mathscr{T}_2^*([\bar{\boldsymbol{v}}_2, q_2]) + \tilde{\mu}_2, \tilde{\gamma} - \tilde{\boldsymbol{u}}_2 \rangle_\Gamma = 0, \tag{14}$$

$$\langle \bar{\boldsymbol{v}}_1 + \bar{\boldsymbol{v}}_2 + \tilde{\kappa}, \mathscr{T}_1([\bar{\boldsymbol{u}}_1, p_1]) + \mathscr{T}_2([\bar{\boldsymbol{u}}_2, p_2]) + \tilde{\lambda}_1 + \tilde{\lambda}_2 \rangle_\Gamma$$
$$+ \langle \bar{\boldsymbol{v}}_1 + \tilde{\kappa}, \mathscr{T}_1([\bar{\boldsymbol{u}}_1, p_1]) + \tilde{\lambda}_N \rangle_{\Gamma_N} = \langle \bar{\boldsymbol{v}}_1 + \tilde{\kappa}, \boldsymbol{t} \rangle_{\Gamma_N}, \tag{15}$$

which must hold for all $\bar{\boldsymbol{v}}_i \in V_i$, $\tilde{\boldsymbol{v}}_i \in \tilde{V}_i$, $q_i \in Q_i$, $\tilde{\kappa} \in \tilde{T}$, $\tilde{\mu}_i \in \tilde{F}_i$ ($i = 1, 2$). Recall that L_1 does not contain the contribution from the Neumann-type boundary condition (4).

Adding up (11) and (12) with $\tilde{\boldsymbol{v}}_1 = \tilde{\boldsymbol{v}}_2 = \boldsymbol{0}$ and using (15) with $\tilde{\kappa} = \boldsymbol{0}$ yields the original variational equation projected onto $\bar{V} \times Q$, that is to say,

$$B([\bar{\boldsymbol{u}}, p], [\bar{\boldsymbol{v}}, q]) + B([\tilde{\boldsymbol{u}}, 0], [\bar{\boldsymbol{v}}, q]) = L([\bar{\boldsymbol{v}}, q]) + \langle \bar{\boldsymbol{v}}, \boldsymbol{t} \rangle_{\Gamma_N}, \tag{16}$$

which holds for all $[\bar{v}, q] \in \bar{V} \times Q$. If we define the operators

$$\mathscr{L}_i([\bar{v}_i, q_i]) := -\mu \Delta \bar{v}_i + \nabla q_i, \quad \mathscr{L}_i^*([\bar{v}_i, q_i]) := -\mu \Delta \bar{v}_i - \nabla q_i,$$

we may write, making use of (13) and (14) with $\tilde{\mu}_1 = \tilde{\mu}_2 = \mathbf{0}$,

$$B([\tilde{u}, 0], [\bar{v}, q]) = \sum_{i=1}^{2} B_i([\tilde{u}_i, 0], [\bar{v}_i, q_i])$$

$$= \sum_{i=1}^{2} \langle \tilde{u}_i, \mathscr{L}_i^*([\bar{v}_i, q_i]) \rangle_{\Omega_i} + \sum_{i=1}^{2} \langle \tilde{\gamma}, \mathscr{T}_i^*([\bar{v}_i, q_i]) \rangle_{\Gamma} + \langle \tilde{\gamma}, \mathscr{T}_1^*([\bar{v}_1, q_1]) \rangle_{\Gamma_N}. \quad (17)$$

Adding up (11) and (12) with $\bar{v}_1 = \bar{v}_2 = \mathbf{0}$, $q_1 = q_2 = 0$ yields, after integration by parts of some terms,

$$\sum_{i=1}^{2} B_i([\bar{u}_i + \tilde{u}_i, p_i], [\tilde{v}_i, 0]) - \sum_{i=1}^{2} \langle \mathscr{T}_i([\bar{u}_i, p_i]) + \tilde{\lambda}_i, \tilde{v}_i \rangle_{\Gamma} - \langle \mathscr{T}_1([\bar{u}_1, p_1]) + \tilde{\lambda}_N, \tilde{v}_1 \rangle_{\Gamma_N}$$

$$= \sum_{i=1}^{2} \langle \mathscr{L}_i([\bar{u}_i, p_i]), \tilde{v}_i \rangle_{\Omega_i} + \sum_{i=1}^{2} B_i([\tilde{u}_i, 0], [\tilde{v}_i, 0]) - \sum_{i=1}^{2} \langle \tilde{\lambda}_i, \tilde{v}_i \rangle_{\Gamma} - \langle \tilde{\lambda}_N, \tilde{v}_1 \rangle_{\Gamma_N}$$

$$= \sum_{i=1}^{2} L_2([\tilde{v}_i, 0]). \quad (18)$$

As an alternative to (11)–(15), the final problem can be obtained from (16), (17), (18), (13) with $[\bar{v}_1, q_1] = [\mathbf{0}, 0]$, (14) with $[\bar{v}_2, q_2] = [\mathbf{0}, 0]$ and (15) with $\bar{v}_1 = \bar{v}_2 = \mathbf{0}$. It reads: find $\bar{u}_i \in \bar{V}_i$, $\tilde{u}_i \in \tilde{V}_i$, $p_i \in Q_i$, $\tilde{\gamma} \in \tilde{T}$, $\tilde{\lambda}_i \in \tilde{F}_i$ $(i = 1, 2)$ such that

$$B([\bar{u}, p], [\bar{v}, q]) + \sum_{i=1}^{2} \langle \tilde{u}_i, \mathscr{L}_i^*([\bar{v}_i, q_i]) \rangle_{\Omega_i} + \sum_{i=1}^{2} \langle \tilde{\gamma}, \mathscr{T}_i^*([\bar{v}_i, q_i]) \rangle_{\Gamma}$$

$$+ \langle \tilde{\gamma}, \mathscr{T}_1^*([\bar{v}_1, q_1]) \rangle_{\Gamma_N} = L([\bar{v}, q]) + \langle \bar{v}, t \rangle_{\Gamma_N}, \quad (19)$$

$$\sum_{i=1}^{2} \langle \mathscr{L}_i([\bar{u}_i, p_i]), \tilde{v}_i \rangle_{\Omega_i} + \sum_{i=1}^{2} B_i([\tilde{u}_i, 0], [\tilde{v}_i, 0]) - \sum_{i=1}^{2} \langle \tilde{\lambda}_i, \tilde{v}_i \rangle_{\Gamma}$$

$$- \langle \tilde{\lambda}_N, \tilde{v}_1 \rangle_{\Gamma_N} = \sum_{i=1}^{2} L_i([\tilde{v}_i, 0]), \quad (20)$$

$$\sum_{i=1}^{2} \langle \tilde{\kappa}, \mathscr{T}_i([\bar{u}_i, p_i]) + \tilde{\lambda}_i \rangle_{\Gamma} + \langle \tilde{\kappa}, \mathscr{T}_1([\bar{u}_1, p_1]) + \tilde{\lambda}_N \rangle_{\Gamma_N} = \langle \tilde{\kappa}, t \rangle_{\Gamma_N}, \quad (21)$$

$$\sum_{i=1}^{2} \langle \tilde{\mu}_i, \tilde{\gamma} - \tilde{u}_i \rangle_{\Gamma} + \langle \tilde{\mu}_1, \tilde{\gamma} - \tilde{u}_1 \rangle_{\Gamma_N} = 0, \quad (22)$$

for all $\bar{v}_i \in V_i$, $\tilde{v}_i \in \tilde{V}_i$, $q_i \in Q_i$, $\tilde{\kappa} \in \tilde{T}$, $\tilde{\mu}_i \in \tilde{F}_i$ $(i = 1, 2)$.

This is the hybrid formulation on which we will base the finite element approximation described in the following. Its importance relies on the fact that *it is the theoretical framework to develop approximations in which $\mathbf{u}$ is split into a contribution that is continuous on Γ and another one that is discontinuous*. In [6], we presented a similar development for the convection–diffusion equation. Now we have detailed this development for the Stokes problem, considering also the presence of Neumann-type boundary conditions.

3. FINITE ELEMENT APPROXIMATION

3.1. Scale splitting

Let $\mathscr{P}_h := \{K\}$ be a finite element partition of the domain Ω of size h, and $V_h \times Q_h$ a finite element space where an approximate solution $[\boldsymbol{u}_h, p_h] \in V_h \times Q_h$ is sought. We assume that V_h is made *of continuous functions*, that is to say, V_h is conforming in V.

Consider the setting of the previous subsection with $\bar{V} = V_h$, and therefore $V = V_h \oplus \tilde{V}$, with $\tilde{V}$ to be defined, and $\boldsymbol{u} = \boldsymbol{u}_h + \tilde{\boldsymbol{u}}$, $\boldsymbol{v} = \boldsymbol{v}_h + \tilde{\boldsymbol{v}}$. The extension of (19)–(22) to multiple subdomains is straightforward. In particular, we will apply it considering each element as a subdomain. No subscript will be used for the functions and operators in play to characterize the element domain over which they are defined, this being clear simply by the domain of integration.

The discrete variational problem to be considered is to find $[\boldsymbol{u}_h, p_h] \in V_h \times Q_h$, $\tilde{\boldsymbol{u}} \in \tilde{V}$, $\tilde{\boldsymbol{\gamma}} \in \tilde{T}$ and $\tilde{\boldsymbol{\lambda}} \in \tilde{F}$ such that

$$B([\boldsymbol{u}_h, p_h], [\boldsymbol{v}_h, q_h]) + \sum_K \langle \tilde{\boldsymbol{u}}, \mathscr{L}^*([\boldsymbol{v}_h, q_h]) \rangle_K$$

$$+ \sum_K \langle \tilde{\boldsymbol{\gamma}}, \mathscr{T}^*([\boldsymbol{v}_h, q_h]) \rangle_{\partial K} = L([\boldsymbol{v}_h, q]) + \langle \boldsymbol{v}_h, \boldsymbol{t} \rangle_{\Gamma_N}, \tag{23}$$

$$\sum_K \langle \mathscr{L}([\boldsymbol{u}_h, p_h]), \tilde{\boldsymbol{v}} \rangle_K + \sum_K B_K([\tilde{\boldsymbol{u}}, 0], [\tilde{\boldsymbol{v}}, 0]) - \sum_K \langle \tilde{\boldsymbol{\lambda}}, \tilde{\boldsymbol{v}} \rangle_{\partial K} = \sum_K L_K([\tilde{\boldsymbol{v}}, 0]), \tag{24}$$

$$\sum_K \langle \tilde{\boldsymbol{\kappa}}, \mathscr{T}([\boldsymbol{u}_h, p_h]) + \tilde{\boldsymbol{\lambda}} \rangle_{\partial K} = \langle \tilde{\boldsymbol{\kappa}}, \boldsymbol{t} \rangle_{\Gamma_N}, \tag{25}$$

$$\sum_K \langle \tilde{\boldsymbol{\mu}}, \tilde{\boldsymbol{\gamma}} - \tilde{\boldsymbol{u}} \rangle_{\partial K} = 0, \tag{26}$$

for all $\boldsymbol{v}_h \in V_h$, $\tilde{\boldsymbol{v}} \in \tilde{V}$, $q_h \in Q_h$, $\tilde{\boldsymbol{\kappa}} \in \tilde{T}$, $\tilde{\boldsymbol{\mu}} \in \tilde{F}$, where $\tilde{T}$ is now the space of traces (of subscales) on the element boundaries (satisfying $\tilde{\boldsymbol{\gamma}} = \boldsymbol{0}$ on Γ_D) and $\tilde{F}$ the space of fluxes on these boundaries.

Apart from the imposition of the condition that $p_h \in Q_h$, problem (23)–(26) is exact. The final approximation is obtained by choosing a way to approximate the velocity subscales $\tilde{\boldsymbol{u}}$, their traces on the element boundaries $\tilde{\boldsymbol{\gamma}}$ and their fluxes $\tilde{\boldsymbol{\lambda}}$. This leaves many possibilities open. In particular, if $\tilde{\boldsymbol{u}}$ is chosen to be a piecewise polynomial, the previous equations constitute a very general framework to develop finite element approximations with a continuous component ($\boldsymbol{u}_h$) and a discontinuous one ($\tilde{\boldsymbol{u}}$). Traces ($\tilde{\boldsymbol{\gamma}}$) and fluxes ($\tilde{\boldsymbol{\lambda}}$) may be approximated independently or linked to $\tilde{\boldsymbol{u}}$ and/or $\boldsymbol{u}_h$ if an irreducible formulation is to be used. Note that if the first option is used, there might be compatibility conditions between the approximating finite element spaces to render the final discrete problem numerically stable.

Our purpose here is *not* to exploit the possibilities of (23)–(26), but *to propose a closed-form expression for $\tilde{\boldsymbol{u}}$, $\tilde{\boldsymbol{\gamma}}$ and $\tilde{\boldsymbol{\lambda}}$*. Only (23) will remain unaltered, but with a certain approximation for $\tilde{\boldsymbol{u}}$ in the interior of the element domains required to evaluate the second term on the left-hand side (LHS) of this equation, and an approximation for $\tilde{\boldsymbol{\gamma}}$ on the element boundaries to evaluate the third term. We proceed to explain how we do this in the following subsection, understanding that other possibilities are open within the present framework.

Let us only remark that if the conforming part of the solution is zero, problem (19)–(22) could serve as a basis to design discontinuous Galerkin approximations for the Stokes problem. It is worth noting that other hybrid formulations can be used as starting points. In particular, in [16] a hybrid formulation is proposed for the diffusion equation, which is extended in [17, 18] to the convection–diffusion equation. The hybridization of the problem is completely different from our three-field approach introduced in [6] for the same problem and applied here to the Stokes problem. To summarize the differences, note that we split the unknown into a continuous and a discontinuous parts, whereas only the latter is used [16–18], and we will give a closed-form expression for the discontinuous part, whereas it is the basic unknown in [16–18]. Moreover, concerning the hybrid formulation, our unknowns are the field in the interior of the elements and its traces and fluxes on
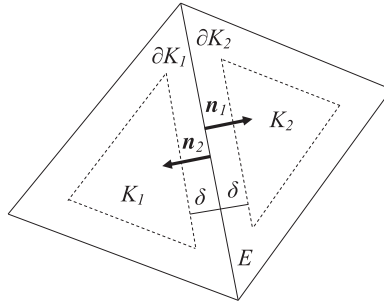
Figure 2. Notation for the approximation of the subscales on the element boundaries.

the boundaries, whereas in the above references it is the unknown and the fluxes in the interior (dual mixed formulation) and the traces on the boundaries. See also [19] for another three-field formulation of the convection–diffusion equation.

3.2. Subscales on the element boundaries

The way we propose to approximate the subscales was already presented in [6]. For completeness, we include it also here, with attention on the treatment of Neumann boundary conditions which will be important in Sections 4 and 5. Let us consider for simplicity the 2D case and the situation depicted in Figure 2, where two elements K_1 and K_2 share an edge E (E stands for 'edge' in 2D or face in 3D). Let $\tilde{u}_i$ be the subscale approximated in the interior of element K_i, $i=1,2$. *We assume that this approximation is valid up to a distance δ to the element boundary*. This distance will be taken of the form $\delta=\delta_0 h$, with $0 \leqslant \delta_0 \leqslant \frac{1}{2}$.

3.2.1. Approximation of $\tilde{\lambda}$. The values of $\tilde{\lambda}$ on ∂K are *weak* approximations to the fluxes of $\tilde{u}$. Given the trace $\tilde{\gamma}$ of this unknown and taking into account that no pressure subscales have been introduced, we propose the following closed-form expression for $\tilde{\lambda}$:

$$\tilde{\lambda}_{\partial K_i \cap E} \approx \frac{\mu}{\delta}(\tilde{\gamma}-\tilde{u}_i), \quad i=1,2, \tag{27}$$

where now $\tilde{u}_i$ has to be understood as the subscale computed in the element interiors and evaluated at edge E. We want to remark that this is the only approximation we really require to compute the subscales on the element boundaries. Obviously, other finite-difference-like approximations to the fluxes of the subscales could be adopted. In particular, if the viscous term is written as the divergence of the symmetrical gradient of the velocities, an approximation for the fluxes of the velocity subscales is not so obvious. In this case, some sort of finite-difference approximation would be needed to approximate $n \cdot \nabla^S \tilde{u}$ (see also Section 5). Finally, it is worth to note that if $\tilde{u}_i$ is assumed to be differentiable within element K_i, (27) could be improved to

$$\tilde{\lambda}_{\partial K_i \cap E} \approx \frac{\mu}{\delta}(\tilde{\gamma}-\tilde{u}_i)+\mu\partial_n\tilde{u}_i, \quad i=1,2,$$

which follows from a Taylor expansion of $\tilde{u}_i$ at the boundary to obtain it at a distance δ from it (see Figure 2), the remainder being $\mathcal{O}(\delta)$. However, we shall not pursue further this improvement in this paper.

3.2.2. Approximation of $\tilde{\gamma}$. Equation (25) states the weak continuity of the total fluxes on the element boundaries. The idea now is to replace this equation by an explicit prescription of this continuity. We need to distinguish the case in which an edge is interior to the domain Ω and the case in which it belongs to Γ_N. Edges on Γ_D will not contribute because of the zero velocity prescription there.

Let $[\![\boldsymbol{n}g]\!]_E := \boldsymbol{n}_1 g|_{\partial K_1 \cap E} + \boldsymbol{n}_2 g|_{\partial K_2 \cap E}$ denote the jump of a scalar function g across edge E and $[\![\partial_n g]\!]_E = \boldsymbol{n}_1 \cdot \nabla g|_{\partial K_1 \cap E} + \boldsymbol{n}_2 \cdot \nabla g|_{\partial K_2 \cap E}$ the jump of the normal derivative. For a vector field $\boldsymbol{v}$, we also define $[\![\boldsymbol{n} \otimes \boldsymbol{v}]\!]_E = \boldsymbol{n}_1 \otimes \boldsymbol{v}|_{\partial K_1 \cap E} + \boldsymbol{n}_2 \otimes \boldsymbol{v}|_{\partial K_2 \cap E}$.

Consider first the case in which E_0 is an interior edge. The condition to determine the expression of the subscale velocity on the boundary is that the normal component of the stress be continuous across interelement boundaries. This can be written as follows:

$$
\begin{aligned}
\mathbf{0} &= [\![-p\boldsymbol{n} + \mu\partial_n \boldsymbol{u}]\!]_{E_0} \\
&\approx [\![-p_h\boldsymbol{n} + \mu\partial_n \boldsymbol{u}_h]\!]_{E_0} + \tilde{\boldsymbol{\lambda}}_{\partial K_1 \cap E_0} + \tilde{\boldsymbol{\lambda}}_{\partial K_2 \cap E_0} \\
&\approx [\![-p_h\boldsymbol{n} + \mu\partial_n \boldsymbol{u}_h]\!]_{E_0} + \frac{\mu}{\delta}\left(2\tilde{\boldsymbol{\gamma}}_{E_0} - \tilde{\boldsymbol{u}}_1 - \tilde{\boldsymbol{u}}_2\right),
\end{aligned}
\tag{28}
$$

from where the approximation we propose is

$$
\boxed{\tilde{\boldsymbol{\gamma}}_{E_0} \approx \{\tilde{\boldsymbol{u}}\}_{E_0} - \frac{\delta}{2\mu}[\![\mu\partial_n \boldsymbol{u}_h - p_h\boldsymbol{n}]\!]_{E_0},}
\tag{29}
$$

where $\{\tilde{\boldsymbol{u}}\}_{E_0} := \frac{1}{2}(\tilde{\boldsymbol{u}}_1 + \tilde{\boldsymbol{u}}_2)$ is the average of the subscales computed in the element interiors evaluated at edge E_0. From (29) it is observed that δ_0 will play the role of an algorithmic parameter for which, following our approach, we have a geometrical interpretation.

From now onwards we will use the symbol $=$ instead of $\approx$, understanding that in some places we perform approximation (27) that has led us to (29).

Let us consider now a boundary edge of the form $E_N = \partial K \cap \Gamma_N$ for a certain element K, where the Neumann condition (4) is prescribed. In this case, (28) has to be replaced by

$$
\begin{aligned}
\boldsymbol{t}|_{E_N} &= (-p\boldsymbol{n} + \mu\partial_n \boldsymbol{u})|_{E_N} \\
&= (-p_h\boldsymbol{n} + \mu\partial_n \boldsymbol{u}_h)|_{E_N} + \mu\partial_n \tilde{\boldsymbol{u}}|_{E_N} \\
&= (-p_h\boldsymbol{n} + \mu\partial_n \boldsymbol{u}_h)|_{E_N} + \frac{\mu}{\delta}(\tilde{\boldsymbol{\gamma}}_{E_N} - \tilde{\boldsymbol{u}}_{E_N}),
\end{aligned}
$$

from where

$$
\boxed{\tilde{\boldsymbol{\gamma}}_{E_N} = \tilde{\boldsymbol{u}}_{E_N} - \frac{\delta}{\mu}(-p_h\boldsymbol{n} + \mu\partial_n \boldsymbol{u}_h - \boldsymbol{t})|_{E_N}.}
\tag{30}
$$

3.2.3. Problem for $\boldsymbol{u}_h$ and $\tilde{\boldsymbol{u}}$. From the approximation of the fluxes (27) and the expressions obtained for the traces, (29) and (30), one can obtain a problem for $\boldsymbol{u}_h$ and $\tilde{\boldsymbol{u}}$ alone from (23) and (24). After some algebraic manipulations, the problem obtained is: find $[\boldsymbol{u}_h, p_h] \in V_h \times Q_h$ and $\tilde{\boldsymbol{u}} \in \tilde{V}$ such that

$$
\begin{aligned}
&B([\boldsymbol{u}_h, p_h], [\boldsymbol{v}_h, q_h]) + \sum_K \langle \tilde{\boldsymbol{u}}, \mathscr{L}^*([\boldsymbol{v}_h, q_h]) \rangle_K \\
&\quad + \sum_{E_0} \langle \{\tilde{\boldsymbol{u}}\}, [\![\mathscr{T}^*([\boldsymbol{v}_h, q_h])]\!] \rangle_{E_0} - \frac{\delta}{2\mu}\sum_{E_0} \langle [\![\mathscr{T}([\boldsymbol{u}_h, p_h])]\!], [\![\mathscr{T}^*([\boldsymbol{v}_h, q_h])]\!] \rangle_{E_0} \\
&\quad + \sum_{E_N} \langle \tilde{\boldsymbol{u}}, \mathscr{T}^*([\boldsymbol{v}_h, q_h]) \rangle_{E_N} - \frac{\delta}{\mu}\sum_{E_N} \langle \mathscr{T}([\boldsymbol{u}_h, p_h]), \mathscr{T}^*([\boldsymbol{v}_h, q_h]) \rangle_{E_N} \\
&= L([\boldsymbol{v}_h, q_h]) + \langle \boldsymbol{v}_h, \boldsymbol{t} \rangle_{\Gamma_N} - \frac{\delta}{\mu}\sum_{E_N} \langle \boldsymbol{t}, \mathscr{T}^*([\boldsymbol{v}_h, q_h]) \rangle_{E_N},
\end{aligned}
\tag{31}
$$

$$
\sum_K B_K([\tilde{\boldsymbol{u}}, 0], [\tilde{\boldsymbol{v}}, 0]) + \sum_K \langle \mathscr{L}([\boldsymbol{u}_h, p_h]), \tilde{\boldsymbol{v}} \rangle_K
$$

$$+\sum_{E_0}\langle[\![\mathscr{T}([\boldsymbol{u}_h,p_h])]\!],\{\tilde{\boldsymbol{v}}\}\rangle_{E_0}+\frac{\delta}{2\mu}\sum_{E_0}\langle[\![\boldsymbol{n}\otimes\tilde{\boldsymbol{u}}]\!],[\![\boldsymbol{n}\otimes\tilde{\boldsymbol{v}}]\!]\rangle_{E_0}$$

$$+\sum_{E_{\mathrm{N}}}\langle\mathscr{T}([\boldsymbol{u}_h,p_h]),\tilde{\boldsymbol{v}}\rangle_{E_{\mathrm{N}}}=\sum_K L_K([\tilde{\boldsymbol{v}},0])+\sum_{E_{\mathrm{N}}}\langle\boldsymbol{t},\tilde{\boldsymbol{v}}\rangle_{E_{\mathrm{N}}},\tag{32}$$

for all $[\boldsymbol{v}_h,q_h]\in V_h\times Q_h$, $\tilde{\boldsymbol{v}}\in\tilde{V}$.

Problem (31)–(32) is very general and could be used as such after choosing an approximation for $\tilde{V}$. However, we will further simplify the problem by approximating directly $\tilde{\boldsymbol{u}}$.

3.3. Subscales in the element interiors

To approximate $\tilde{\boldsymbol{u}}$, we in fact approximate (24) by integrating by parts,

$$\sum_K B_K([\tilde{\boldsymbol{u}},0],[\tilde{\boldsymbol{v}},0])=-\mu\sum_K\langle\Delta\tilde{\boldsymbol{u}},\tilde{\boldsymbol{v}}\rangle_K+\mu\sum_K\langle\boldsymbol{n}\cdot\nabla\tilde{\boldsymbol{u}},\tilde{\boldsymbol{v}}\rangle_{\partial K},$$

assuming that $\mu\boldsymbol{n}\cdot\nabla\tilde{\boldsymbol{u}}$ cancels with the fluxes $\tilde{\boldsymbol{\lambda}}$ and using the crucial approximation

$$\langle-\mu\Delta\tilde{\boldsymbol{u}},\tilde{\boldsymbol{v}}\rangle_K\approx\tau^{-1}\langle\tilde{\boldsymbol{u}},\tilde{\boldsymbol{v}}\rangle_K,\quad\tau^{-1}=C_1\frac{\mu}{h^2},\tag{33}$$

where C_1 is an algorithmic constant. We will not justify this last step, which is the keystone of stabilized finite element methods. It can be motivated, for example, using an approximate Fourier analysis [20].

Summarizing, the subscales in the element interiors can be expressed in terms of $[\boldsymbol{u}_h,p_h]$ from the equation

$$\sum_K\langle\mathscr{L}([\boldsymbol{u}_h,p_h]),\tilde{\boldsymbol{v}}\rangle_K+\tau^{-1}\sum_K\langle\tilde{\boldsymbol{u}},\tilde{\boldsymbol{v}}\rangle_K=\rho\sum_K\langle\boldsymbol{f},\tilde{\boldsymbol{v}}\rangle_K,\tag{34}$$

which can be described by saying that $\tilde{\boldsymbol{u}}$ is the projection of the residual $\rho\boldsymbol{f}-\mathscr{L}([\boldsymbol{u}_h,p_h])$ within each element multiplied by τ onto the space of subscales $\tilde{V}$. The most usual option is to take this projection as the identity (assuming this is feasible), although we favor the choice of taking it as the projection L^2-orthogonal to the finite element space V_h. This leads to the so-called orthogonal subscale stabilization (OSS) method [20, 21]. However, the final method is independent of the choice of the space of subscales.

3.4. Stabilized finite element problem

With all the approximations introduced, the problem to be solved consists of (31) and (34). However, the approximations used to arrive to (34) have as a consequence the loss of symmetry of the problem (which is in fact observed using $-q_h$ as test function). This symmetry can be recovered neglecting the third and fifth terms in (31). Note that this maintains the consistency of the method, in the sense that if the approximate solution $[\boldsymbol{u}_h,p_h]$ is replaced by the exact solution $[\boldsymbol{u},p]$, the discrete variational problem holds exactly.

In [6] it is shown that (31) and (34) are stable (when there are no Neumann boundary conditions). Here, however, we will restrict ourselves to the variation of the method just explained, which consists of finding $[\boldsymbol{u}_h,p_h]\in V_h\times Q_h$ and $\tilde{\boldsymbol{u}}\in\tilde{V}$ such that

$$B([\boldsymbol{u}_h,p_h],[\boldsymbol{v}_h,q_h])+\sum_K\langle\tilde{\boldsymbol{u}},\mathscr{L}^*([\boldsymbol{v}_h,q_h])\rangle_K$$

$$-\frac{\delta}{2\mu}\sum_{E_0}\langle[\![\mathscr{T}([\boldsymbol{u}_h,p_h])]\!],[\![\mathscr{T}^*([\boldsymbol{v}_h,q_h])]\!]\rangle_{E_0}-\frac{\delta}{\mu}\sum_{E_{\mathrm{N}}}\langle\mathscr{T}([\boldsymbol{u}_h,p_h]),\mathscr{T}^*([\boldsymbol{v}_h,q_h])\rangle_{E_{\mathrm{N}}}$$

$$=L([\boldsymbol{v}_h,q_h])+\langle\boldsymbol{v}_h,\boldsymbol{t}\rangle_{\Gamma_{\mathrm{N}}}-\frac{\delta}{\mu}\sum_{E_{\mathrm{N}}}\langle\boldsymbol{t},\mathscr{T}^*([\boldsymbol{v}_h,q_h])\rangle_{E_{\mathrm{N}}},\tag{35}$$

$$\sum_K\langle\mathscr{L}([\boldsymbol{u}_h,p_h]),\tilde{\boldsymbol{v}}\rangle_K+\tau^{-1}\sum_K\langle\tilde{\boldsymbol{u}},\tilde{\boldsymbol{v}}\rangle_K=\rho\sum_K\langle\boldsymbol{f},\tilde{\boldsymbol{v}}\rangle_K,\tag{36}$$

for all $[\boldsymbol{v}_h,q_h]\in V_h\times Q_h$, $\tilde{\boldsymbol{v}}\in\tilde{V}$.

We may write the solution of (36) as

$$\tilde{\boldsymbol{u}} = \tilde{P}(\rho\boldsymbol{f} - \mathscr{L}([\boldsymbol{u}_h, p_h])),$$

where $\tilde{P}$ denotes the L^2 projection onto the space of subscales, which will be left undefined (except in the numerical examples, of course). The problem can now be written in a compact form, only involving the finite element component of the unknown $[\boldsymbol{u}_h, p_h]$, as follows: find $[\boldsymbol{u}_h, p_h] \in V_h \times Q_h$ such that

$$B_{\text{stab}}([\boldsymbol{u}_h, p_h], [\boldsymbol{v}_h, q_h]) = L_{\text{stab}}([\boldsymbol{v}_h, q_h]) \quad \forall [\boldsymbol{v}_h, q_h] \in V_h \times Q_h,$$

where

$$B_{\text{stab}}([\boldsymbol{u}_h, p_h], [\boldsymbol{v}_h, q_h]) = B([\boldsymbol{u}_h, p_h], [\boldsymbol{v}_h, q_h]) - \sum_K \tau \langle \tilde{P}(\mathscr{L}([\boldsymbol{u}_h, p_h])), \mathscr{L}^*([\boldsymbol{v}_h, q_h]) \rangle_K$$

$$- \frac{\delta}{2\mu} \sum_{E_0} \langle [\![\mathscr{T}([\boldsymbol{u}_h, p_h])]\!], [\![\mathscr{T}^*([\boldsymbol{v}_h, q_h])]\!] \rangle_{E_0}$$

$$- \frac{\delta}{\mu} \sum_{E_{\text{N}}} \langle \mathscr{T}([\boldsymbol{u}_h, p_h]), \mathscr{T}^*([\boldsymbol{v}_h, q_h]) \rangle_{E_{\text{N}}}, \tag{37}$$

$$L_{\text{stab}}([\boldsymbol{v}_h, q_h]) = L([\boldsymbol{v}_h, q_h]) + \langle \boldsymbol{v}_h, \boldsymbol{t} \rangle_{\Gamma_{\text{N}}} - \sum_K \tau \langle \tilde{P}(\rho\boldsymbol{f}), \mathscr{L}^*([\boldsymbol{v}_h, q_h]) \rangle_K$$

$$- \frac{\delta}{\mu} \sum_{E_{\text{N}}} \langle \boldsymbol{t}, \mathscr{T}^*([\boldsymbol{v}_h, q_h]) \rangle_{E_{\text{N}}}. \tag{38}$$

The stability analysis of this scheme in an adequate norm can be performed using the same strategy as in [6]. The terms included to deal properly with Neumann boundary conditions do not offer any additional difficulty and, moreover, the terms that have been neglected even simplify this analysis. Once stability is established, and taking into account that the method is consistent in the sense explained earlier, convergence follows easily. It is not our purpose here to detail this numerical analysis.

4. INTERACTION BETWEEN SUBDOMAINS

4.1. Motivation

The stabilized finite element formulation presented in the previous section has been designed to allow arbitrary velocity–pressure interpolations, in particular discontinuous pressures. However, the concepts used to obtain it can be applied to other situations. In particular, we consider in this section the application to the interaction between two subdomains, in both of which the Stokes problem is solved.

The motivation to use the stabilization strategy in interaction problems arises from the fact that if the subdomains are discretized independently, the pressure degrees of freedom at the interface will be doubled and, therefore, pressure will be discontinuous at this interface. If a method that is stable for continuous pressures is applied (either coming from a stabilized formulation or from the use of inf–sup stable velocity–pressure pairs), there is no guarantee that this stability will be preserved at the interface. The use of the approach described in the previous section, known to be stable for arbitrary pressure interpolations, may thus be beneficial.

4.2. Continuous problem

The final discrete problem to be proposed can be derived directly using the ideas presented in the previous section and extended to the case in which the physical properties, and in particular the viscosity μ, are discontinuous. However, additional insight into the method is gained if a more 'physical' approach is used when two subdomains interact.

Let us consider again the situation of Figure 1, now for simplicity with $\Gamma_N = \emptyset$. For our purposes, instead of using a three-field hybrid formulation, using the primal unknown, its traces and its fluxes as variables, it is enough to consider the more common approach of using only the fluxes on Γ as unknowns, and enforcing continuity weakly. The boundary value problem to be solved consists of finding $[\boldsymbol{u}_1, p_1]$, $[\boldsymbol{u}_2, p_2]$ and $\boldsymbol{\lambda}$ such that

$$-\mu_1 \Delta \boldsymbol{u}_1 + \nabla p_1 = \rho \boldsymbol{f} \quad \text{in } \Omega_1,$$

$$\nabla \cdot \boldsymbol{u}_1 = 0 \quad \text{in } \Omega_1,$$

$$\boldsymbol{u}_1 = \boldsymbol{0} \quad \text{on } \Gamma_{D,1} = \partial \Omega_1 \cap \partial \Omega,$$

$$\boldsymbol{u}_1 = \boldsymbol{u}_2 \quad \text{on } \Gamma,$$

$$\boldsymbol{\lambda} = -p_1 \boldsymbol{n}_1 + \mu_1 \boldsymbol{n}_1 \cdot \nabla \boldsymbol{u}_1 \quad \text{on } \Gamma,$$

$$-\mu_2 \Delta \boldsymbol{u}_2 + \nabla p_2 = \rho \boldsymbol{f} \quad \text{in } \Omega_2,$$

$$\nabla \cdot \boldsymbol{u}_2 = 0 \quad \text{in } \Omega_2,$$

$$\boldsymbol{u}_2 = \boldsymbol{0} \quad \text{on } \Gamma_{D,2} = \partial \Omega_2 \cap \partial \Omega,$$

$$-p_2 \boldsymbol{n}_2 + \mu_2 \boldsymbol{n}_2 \cdot \nabla \boldsymbol{u}_2 = -\boldsymbol{\lambda} \quad \text{on } \Gamma.$$

These equations have been written in the order they can be solved in an iteration-by-subdomain strategy. The first four equations can be solved for $[\boldsymbol{u}_1, p_1]$ if $\boldsymbol{u}_2$ is assumed to be known on Γ, the flux on this surface can be then computed and used to solve the problem on Ω_2 with Neumann conditions on Γ.

The variational form of the continuous problem consists of finding $[\boldsymbol{u}_1, p_1]$, $[\boldsymbol{u}_2, p_2]$ and $\boldsymbol{\lambda}$ such that

$$B_1([\boldsymbol{u}_1, p_1], [\boldsymbol{v}_1, q_1]) - \langle \boldsymbol{\lambda}, \boldsymbol{v}_1 \rangle_\Gamma = L_1([\boldsymbol{v}_1, q_1]) \quad \forall [\boldsymbol{v}_1, q_1],$$

$$B_2([\boldsymbol{u}_2, p_2], [\boldsymbol{v}_2, q_2]) + \langle \boldsymbol{\lambda}, \boldsymbol{v}_2 \rangle_\Gamma = L_2([\boldsymbol{v}_2, q_2]) \quad \forall [\boldsymbol{v}_2, q_2],$$

$$\langle \boldsymbol{\mu}, \boldsymbol{u}_1 - \boldsymbol{u}_2 \rangle_\Gamma = 0 \quad \forall \boldsymbol{\mu},$$

where the bilinear and linear forms involved are the same as in the previous section. The spaces of unknowns and test functions are also the same as those introduced previously.

When applying the Galerkin method to discretize this problem, there are at least two issues that have to be taken into account:

- The space for $\boldsymbol{\lambda}$ has to be properly chosen in order to obtain a numerically stable problem. There are compatibility conditions between the interpolation of this unknown and the interpolation of $\boldsymbol{u}$ and p that have to be met to satisfy the inf–sup conditions associated with the problem.
- It is preferable to compute $\boldsymbol{\lambda}_h$ *weakly* rather than from $\boldsymbol{\lambda} = -p_1 \boldsymbol{n}_1 + \mu_1 \boldsymbol{n}_1 \cdot \nabla \boldsymbol{u}_1$.

However, it is not our purpose to use the classical Galerkin method, but to extend the formulation of Section 3.

4.3. Finite element approximation

Let $B_{1,\text{stab}}$, $L_{1,\text{stab}}$, $B_{2,\text{stab}}$ and $L_{2,\text{stab}}$ be the stabilized bilinear and linear forms corresponding to each subdomain *without* considering the boundary conditions on Γ, which act as Neumann conditions on each subdomain. These forms are given by (37) and (38).

If $\boldsymbol{t}_i$ is the traction on Γ to be applied to Ω_i, the discrete variational equation on each subdomain reads:

$$B_{i,\text{stab}}([\boldsymbol{u}_h, p_h], [\boldsymbol{v}_h, q_h]) - \frac{\delta}{\mu_i} \sum_{E_\Gamma} \langle \mathcal{T}_i([\boldsymbol{u}_h, p_h]), \mathcal{T}_i^*([\boldsymbol{v}_h, q_h]) \rangle_{E_\Gamma}$$

$$= L_{i,\text{stab}}([\boldsymbol{v}_h, q_h]) + \langle \boldsymbol{t}_i, \boldsymbol{v}_h \rangle_\Gamma - \frac{\delta}{\mu_i} \sum_{E_\Gamma} \langle \boldsymbol{t}_i, \mathcal{T}_i^*([\boldsymbol{v}_h, q_h]) \rangle_{E_\Gamma}, \tag{39}$$

which holds for all test functions $[\boldsymbol{v}_h, q_h]$ with support on Ω_i, $i = 1, 2$. The edges E_Γ are now those contained in Γ.

Let us obtain the traction $\boldsymbol{t}_i$ that results from the formulation developed in the previous section. Note that $\boldsymbol{t}_1 = -\lambda_2$ and $\boldsymbol{t}_2 = -\lambda_1$. Recall that we have neglected the subscales in the element interiors (and evaluated on the boundary) when computing the fluxes $\tilde{\boldsymbol{\lambda}}$.

If the continuity of fluxes (28) is now imposed, we find

$$\tilde{\gamma}|_{E_\Gamma} = -\frac{\delta}{\mu_1 + \mu_2} [\![\, \mathscr{T}([\boldsymbol{u}_h, p_h]) \,]\!]_{E_\Gamma}.$$

Using the basic decomposition assumed for the total fluxes and (27) we obtain, on each edge E_Γ,

$$\lambda_i = \mathscr{T}_i([\boldsymbol{u}_h, p_h]) + \tilde{\lambda}_i = \mathscr{T}_i([\boldsymbol{u}_h, p_h]) + \frac{\mu_i}{\delta}\tilde{\gamma}.$$

Combining the last two expressions yields, on each edge E_Γ,

$$\lambda_i = \mathscr{T}_i([\boldsymbol{u}_h, p_h]) - \frac{\mu_i}{\mu_1 + \mu_2} [\![\, \mathscr{T}([\boldsymbol{u}_h, p_h]) \,]\!]. \tag{40}$$

This expression for the traction associated with the formulation we propose has two interesting features:

- It *automatically* satisfies $\lambda_1 + \lambda_2 = \boldsymbol{0}$.
- Instead of the traction $\mathscr{T}_i([\boldsymbol{u}_h, p_h])$ associated with the standard Galerkin method, λ_i is a *weighted average* of $\mathscr{T}_1([\boldsymbol{u}_h, p_h])$ and $\mathscr{T}_2([\boldsymbol{u}_h, p_h])$, the weighting coefficients depending on the viscosity on each subdomain. If $i = 1$, for example, we see that

$$\lambda_1 = \frac{\mu_2}{\mu_1 + \mu_2} \mathscr{T}_1([\boldsymbol{u}_h, p_h]) + \frac{\mu_1}{\mu_1 + \mu_2}(-\mathscr{T}_2([\boldsymbol{u}_h, p_h])),$$

where $-\mathscr{T}_2([\boldsymbol{u}_h, p_h])$ can be understood as the traction associated with $[\boldsymbol{u}_h, p_h]$ in Ω_2 but computed with the normal $\boldsymbol{n}_1$.

It is worth to remark that (40) can be used to compute the fluxes in domain interaction problems as an alternative to the classical fluxes of the Galerkin method and also to the weak computation of these fluxes. It can be used not only in the case of meshes that match on Γ, but also in domain decomposition methods with overlapping [22] or when fluxes are needed on meshes that do not match the boundaries [23]. Likewise, they can be modified to accommodate particular conditions that a certain application requires, such as conservation of angular momentum (using, for example, the methodology proposed in [24]).

The formulation we propose can finally be obtained adding up (39) for $i = 1$ and $i = 2$. Writing explicitly the expressions of $\mathscr{T}([\boldsymbol{u}_h, p_h])$ and $\mathscr{T}^*([\boldsymbol{v}_h, q_h])$, it consists of finding $[\boldsymbol{u}_h, p_h]$, defined on the whole computational domain Ω, such that

$$B_{1,\text{stab}}([\boldsymbol{u}_h, p_h], [\boldsymbol{v}_h, q_h]) + B_{2,\text{stab}}([\boldsymbol{u}_h, p_h], [\boldsymbol{v}_h, q_h])$$

$$- \sum_{E_\Gamma} \frac{\delta}{\mu_1 + \mu_2} \langle [\![\, \mu \partial_n \boldsymbol{u}_h - p_h \boldsymbol{n} \,]\!], [\![\, \mu \partial_n \boldsymbol{v}_h + q_h \boldsymbol{n} \,]\!] \rangle_{E_\Gamma}$$

$$= L_{1,\text{stab}}([\boldsymbol{v}_h, q_h]) + L_{2,\text{stab}}([\boldsymbol{v}_h, q_h]), \tag{41}$$

for all test functions $[\boldsymbol{v}_h, q_h]$. It is observed that the term involving integrals over Γ penalizes the jump of the (pseudo-) tractions along this interface. We will observe this effect in the numerical examples.
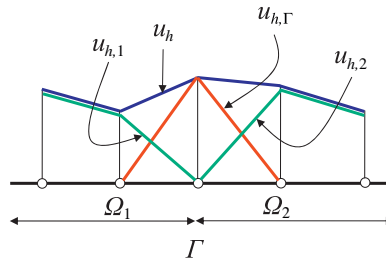
Figure 3. Splitting of the unknown.

4.4. Matrix structure

In order to write the matrix structure of problem (41), consider the splitting of the finite element velocity

$$\boldsymbol{u}_h = \boldsymbol{u}_{h,1} + \boldsymbol{u}_{h,\Gamma} + \boldsymbol{u}_{h,2},$$

where $\boldsymbol{u}_{h,i}$ refers to the component associated with the degrees of freedom *internal* to Ω_i, and vanishing on Γ, whereas $\boldsymbol{u}_{h,\Gamma}$ refers precisely to the degrees of freedom associated with the interacting boundary. This splitting in the 1-D case and using linear elements is represented in Figure 3. For the pressure, $p_{h,i}$ denotes simply its restriction to Ω_i.

Having introduced this splitting, the matrix structure of the problem will be:

$$\begin{bmatrix} A_{1,1} & A_{1,\Gamma} + A'_{1,\Gamma} & A''_{1,2} \\ A_{\Gamma,1} + A'_{\Gamma,1} & A_{\Gamma,\Gamma} + A'_{\Gamma,\Gamma} & A_{\Gamma,2} + A'_{\Gamma,2} \\ A''_{2,1} & A_{2,\Gamma} + A'_{2,\Gamma} & A_{2,2} \end{bmatrix} \begin{bmatrix} U_1 \\ U_\Gamma \\ U_2 \end{bmatrix} = \begin{bmatrix} F_1 \\ F_\Gamma \\ F_2 \end{bmatrix}. \tag{42}$$

In this equation, U_i are arrays of degrees of freedom associated with $\boldsymbol{u}_{h,i}$ and $p_{h,i}$, and U_Γ the degrees of freedom associated with $\boldsymbol{u}_{h,\Gamma}$. The terms from where the different submatrices and components of the right-hand side (RHS) appear are obvious.

There are two remarks to be made referred to the algebraic problem (42):

- Submatrices with a prime and a double prime are due to the *new interaction term* in (41), which would not appear using a classical Gakerkin method for the domain interaction problem (even if stabilized finite element formulations are used within each subdomain).
- $A''_{1,2}$ and $A''_{2,1}$ appear *because of the jump of the derivatives* of the velocities. For example, there are test functions in Ω_1 that vanish on Γ but whose derivative does not vanish (in the case of Lagrangian interpolations, those are the test functions associated with the nodes adjacent to Γ). Thus, the jump of these derivatives is not zero and has to be multiplied against the jump of the velocity derivatives, which involves degrees of freedom of $\boldsymbol{u}_h$ *interior* to Ω_2 (again, in the case of Lagrangian interpolations, those are the velocity degrees of freedom associated with the nodes adjacent to Γ in the interior of Ω_2).

4.5. Iteration-by-subdomain strategy

The most popular way to deal with a problem involving the interaction of two subdomains is using an iteration-by-subdomain strategy, that is to say, an iterative algorithm in which the unknowns are computed in one of the subdomains assuming the data from the other known, and proceeding iteratively until convergence.

To set possible iteration-by-subdomain schemes, it is convenient to consider first the matrix version of the problem. The simplest way to solve (42) is to solve for U_1 first and for U_Γ and U_2 in a coupled way. Denoting with a superscript the iteration counter, a solve of this iterative

algorithm would be:

$$A_{1,1}U_1^{(i)} = F_1 - (A_{1,\Gamma} + A'_{1,\Gamma})U_\Gamma^{(i-1)} - A''_{1,2}U_2^{(i-1)}, \tag{43}$$

$$\begin{bmatrix} A_{\Gamma,\Gamma} + A'_{\Gamma,\Gamma} & A_{\Gamma,2} + A'_{\Gamma,2} \\ A_{2,\Gamma} + A'_{2,\Gamma} & A_{2,2} \end{bmatrix} \begin{bmatrix} U_\Gamma^{(i)} \\ U_2^{(i)} \end{bmatrix} = \begin{bmatrix} F_\Gamma - (A_{\Gamma,1} + A'_{\Gamma,1})U_1^{(i)} \\ F_2 - A''U_1^{(i)} \end{bmatrix}. \tag{44}$$

This scheme would in fact be of Gauss–Seidel type, since the value of U_1 just computed in the first step of the iteration is used in the second. A Jacobi-type scheme would be obtained replacing $U_1^{(i)}$ by $U_1^{(i-1)}$ in the second step.

Apart from the straightforward scheme (43)–(44), there are extensions and/or modifications that are convenient to use in the applications:

- Under-relaxation. Numerical experiments show that it is crucial to use under-relaxation. A simple scheme of the form

$$U_k^{(i)} \leftarrow \alpha U_k^{(i)} + (1-\alpha)U_k^{(i-1)} \tag{45}$$

turns out to be very efficient. The values of the relaxation parameter α that we use are indicated in the numerical examples.

- Other iterative schemes, like GMRES. In principle, this type of schemes can be applied directly to (42) with an adequate choice of the preconditioner P. The key issue is to design this preconditioner in a modular way, that is to say, in such a manner that it requires only information of the domain whose unknowns are being computed. Our choice for the preconditioner P is:

$$P = \begin{bmatrix} A_{1,1} & A_{1,\Gamma} + A'_{1,\Gamma} & 0 \\ A_{\Gamma,1} + A'_{\Gamma,1} & A_{\Gamma,\Gamma} + A'_{\Gamma,\Gamma} & 0 \\ 0 & 0 & A_{22} \end{bmatrix},$$

which leads to the following preconditioned system:

$$AP^{-1}PU = F. \tag{46}$$

The only system of equations to be solved in the GMRES iteration is the one associated with P^{-1}, in which we can separate terms associated with the problem in domain 1 from terms associated with the problem in domain 2 (see also [12, 13]).

The iterative scheme is better described using the algebraic form of the problem, but it is also enlightening to write the discrete variational version. The problem corresponding to (43)–(44) applied to (41) is:

$$B_{1,\text{stab}}([\boldsymbol{u}_{h,1}^{(i)}, p_{h,1}^{(i)}], [\boldsymbol{v}_{h,1}, q_{h,1}])$$

$$= L_{1,\text{stab}}([\boldsymbol{v}_{h,1}, q_{h,1}]) - B_{1,\text{stab}}([\boldsymbol{u}_{h,\Gamma}^{(i-1)}, 0], [\boldsymbol{v}_{h,1}, q_{h,1}]))$$

$$+ \sum_{E_\Gamma} \frac{\delta}{\mu_1 + \mu_2} \langle \mu_1 \partial_{n_1}(\boldsymbol{u}_{h,1}^{(i)} + \boldsymbol{u}_{h,\Gamma}^{(i-1)}) - p_{h,1}^{(i)}\boldsymbol{n}_1, \mu_1 \partial_{n_1}\boldsymbol{v}_{h,1} + q_{h,1}\boldsymbol{n}_1 \rangle_{E_\Gamma}$$

$$+ \sum_{E_\Gamma} \frac{\delta}{\mu_1 + \mu_2} \langle \mu_2 \partial_{n_2} (\boldsymbol{u}_{h,\Gamma}^{(i-1)} + \boldsymbol{u}_{h,2}^{(i-1)}) - p_{h,2}^{(i-1)} \boldsymbol{n}_2, \mu_1 \partial_{n_1} \boldsymbol{v}_{h,1} + q_{h,1} \boldsymbol{n}_1 \rangle_{E_\Gamma},$$

$$B_{2,\text{stab}}([\boldsymbol{u}_{h,\Gamma}^{(i)} + \boldsymbol{u}_{h,2}^{(i)}, p_{h,2}^{(i)}], [\boldsymbol{v}_{h,\Gamma} + \boldsymbol{v}_{h,2}, q_{h,2}])$$

$$= L_{2,\text{stab}}([\boldsymbol{v}_{h,\Gamma} + \boldsymbol{v}_{h,2}, q_{h,2}]) - B_{2,\text{stab}}([\boldsymbol{u}_{h,1}^{(i)}, p_{h,1}^{(i)}], [\boldsymbol{v}_{h,\Gamma} + \boldsymbol{v}_{h,2}, q_{h,2}])$$

$$+ \sum_{E_\Gamma} \frac{\delta}{\mu_1 + \mu_2} \langle \mu_1 \partial_{n_1} (\boldsymbol{u}_{h,1}^{(i)} + \boldsymbol{u}_{h,\Gamma}^{(i)}) - p_{h,1}^{(i)} \boldsymbol{n}_1, \mu_1 \partial_{n_1} \boldsymbol{v}_{h,\Gamma} \rangle_{E_\Gamma}$$

$$+ \sum_{E_\Gamma} \frac{\delta}{\mu_1 + \mu_2} \langle \mu_2 \partial_{n_2} (\boldsymbol{u}_{h,\Gamma}^{(i)} + \boldsymbol{u}_{h,2}^{(i)}) - p_{h,2}^{(i)} \boldsymbol{n}_2, \mu_1 \partial_{n_1} \boldsymbol{v}_{h,\Gamma} \rangle_{E_\Gamma}$$

$$+ \sum_{E_\Gamma} \frac{\delta}{\mu_1 + \mu_2} \langle \mu_1 \partial_{n_1} (\boldsymbol{u}_{h,1}^{(i)} + \boldsymbol{u}_{h,\Gamma}^{(i)}) - p_{h,1}^{(i)} \boldsymbol{n}_1, \mu_2 \partial_{n_2} (\boldsymbol{v}_{h,\Gamma} + \boldsymbol{v}_{h,2}) + q_{h,2} \boldsymbol{n}_2 \rangle_{E_\Gamma}$$

$$+ \sum_{E_\Gamma} \frac{\delta}{\mu_1 + \mu_2} \langle \mu_2 \partial_{n_2} (\boldsymbol{u}_{h,\Gamma}^{(i)} + \boldsymbol{u}_{h,2}^{(i)}) - p_{h,2}^{(i)} \boldsymbol{n}_2, \mu_2 \partial_{n_2} (\boldsymbol{v}_{h,\Gamma} + \boldsymbol{v}_{h,2}) + q_{h,2} \boldsymbol{n}_2 \rangle_{E_\Gamma}.$$

5. FLUID–STRUCTURE INTERACTION

In the previous section we have considered the interaction between two subdomains in both of which the Stokes problem is solved. In this sense, the situation can be considered as a *homogeneous* interaction. The problem to be solved in each subdomain is (39) and, since these equations are dimensionally homogeneous, they can be added up for $i = 1, 2$ to obtain (41). In this section, however, we are interested in the interaction between a *fluid* and a *solid*, and thus the problem can be termed as *heterogeneous*. In this case, it is better to work directly with (39). The purpose of what follows is to apply the ideas introduced previously to FSI problems and to design an iteration-by-subdomain strategy for this particular problem.

5.1. Continuous problem

The nature of the problem to be considered is intrinsically transient (although it is obviously possible that a steady-state is reached). Let $[0, T]$ be the time interval of analysis. In all what follows, we will use subscript F to refer to the fluid and subscript S to refer to the solid (and not subscripts 1 and 2, as in the previous section). In particular, Ω_F and Ω_S will be the subdomains occupied by the fluid and the solid, respectively, and $\Gamma = \partial \bar{\Omega}_F \cap \partial \bar{\Omega}_S$ their common boundary.

If $\boldsymbol{d} : [0, T] \times \Omega_S \longrightarrow \mathbb{R}^d$ is the displacement field in the solid, the problem to be solved consists of finding $\boldsymbol{d}, \boldsymbol{u}$ and p such that

$$\rho_S \partial_{tt}^2 \boldsymbol{d} - \nabla \cdot \boldsymbol{\sigma}_S = \rho_S \boldsymbol{f} \quad \text{in } \Omega_S,$$

$$\boldsymbol{d} = \boldsymbol{0} \quad \text{on } \Gamma_{D_S},$$

$$\boldsymbol{n}_S \cdot \boldsymbol{\sigma}_S = \boldsymbol{t}_S \quad \text{on } \Gamma_{N_S},$$

$$\rho_F \partial_t \boldsymbol{u} - \mu \Delta \boldsymbol{u} + \nabla p = \rho_F \boldsymbol{f} \quad \text{in } \Omega_F,$$

$$\nabla \cdot \boldsymbol{u} = 0 \quad \text{in } \Omega_F,$$

$$\boldsymbol{u} = \boldsymbol{0} \quad \text{on } \Gamma_{D_N},$$

$$-p \boldsymbol{n}_F + \mu \boldsymbol{n}_F \cdot \nabla \boldsymbol{u} = \boldsymbol{t}_F \quad \text{on } \Gamma_{N_F},$$

$$\boldsymbol{n}_S \cdot \boldsymbol{\sigma}_S + (-p \boldsymbol{n}_F + \mu \boldsymbol{n}_F \cdot \nabla \boldsymbol{u}) = \boldsymbol{0} \quad \text{on } \Gamma,$$

$$\partial_t \boldsymbol{d} - \boldsymbol{u} = \boldsymbol{0} \quad \text{on } \Gamma,$$

together with initial conditions for $\boldsymbol{u}$, $\boldsymbol{d}$ and $\partial_t \boldsymbol{d}$ in the domain where they are defined. A linear elastic behavior will be assumed for the solid, so that the stress tensor there is given by

$$\boldsymbol{\sigma}_S = \boldsymbol{\sigma}_S(\boldsymbol{d}) = \boldsymbol{C} : \nabla^S \boldsymbol{d},$$

where $\boldsymbol{C}$ is the constitutive tensor and $\nabla^S \boldsymbol{d}$ the symmetrical gradient of $\boldsymbol{d}$. For simplicity, the non-linear convective term has been neglected in the modeling of the fluid.

Also to simplify the exposition, we assume that the solid is *not* incompressible, so that the problem can be approximated without the need to introduce the volumetric stress as a new variable (the extension to this situation would be straightforward and, in fact, we use it in the numerical examples). Therefore, the standard Galerkin method can be used to approximate the governing equations for the solid.

The variational counterpart of the FSI problem consists of finding $\boldsymbol{d}, \boldsymbol{u}, p$ and the interaction stress $\boldsymbol{\lambda}$ such that

$$\rho_S(\partial_{tt}^2 \boldsymbol{d}, \boldsymbol{e})_{\Omega_S} + B_S(\boldsymbol{d}, \boldsymbol{e}) - \langle \boldsymbol{\lambda}, \boldsymbol{e} \rangle_\Gamma = L_S(\boldsymbol{e}) + \langle \boldsymbol{t}_S, \boldsymbol{e} \rangle_{\Gamma_{N_S}} \quad \forall \boldsymbol{e} \in W,$$

$$\rho_F(\partial_t \boldsymbol{u}, \boldsymbol{v})_{\Omega_F} + B_F([\boldsymbol{u}, p], [\boldsymbol{v}, q]) + \langle \boldsymbol{\lambda}, \boldsymbol{v} \rangle_\Gamma = L_F([\boldsymbol{v}, q]) + \langle \boldsymbol{t}_F, \boldsymbol{v} \rangle_{\Gamma_{N_F}} \quad \forall [\boldsymbol{v}, q] \in V \times Q,$$

$$\langle \boldsymbol{\mu}, \partial_t \boldsymbol{d} - \boldsymbol{u} \rangle_\Gamma = 0 \quad \forall \boldsymbol{\mu} \in F,$$

where

$$W = \{\boldsymbol{e} \in H^1(\Omega_S)^d | \boldsymbol{e} = \boldsymbol{0} \text{ on } \Gamma_{D_S}\},$$

$$B_S(\boldsymbol{d}, \boldsymbol{e}) = (\boldsymbol{C} : \nabla^S \boldsymbol{d}, \nabla^S \boldsymbol{e})_{\Omega_S},$$

$$L_S(\boldsymbol{e}) = \rho_S \langle \boldsymbol{f}, \boldsymbol{e} \rangle_{\Omega_S},$$

and for each time $t \in (0, T)$ the unknowns satisfy $\boldsymbol{d} \in W$, $[\boldsymbol{u}, p] \in V \times Q$, $\boldsymbol{\lambda} \in F$ (with the adequate regularity in time), with the appropriate initial conditions at $t = 0$.

5.2. Finite element approximation and interaction stresses

Once finite element spaces $W_h \subset W$, $V_h \times Q_h \subset V \times Q$ are chosen, the crucial issue is to extend the formulation of the previous section to the present FSI problem to obtain the interaction stresses resulting from the introduction of subscales on the element boundaries contained in Γ. Let $\mathscr{T}_S(\boldsymbol{e}) = \boldsymbol{n}_S \cdot \boldsymbol{\sigma}_S(\boldsymbol{e})$. The velocity subscales $\tilde{\gamma}_F$ and the displacement subscales $\tilde{\gamma}_S$ can be obtained from condition (28), which now can be written as follows:

$$\boldsymbol{0} = \mathscr{T}_F([\boldsymbol{u}, p]) + \mathscr{T}_S(\boldsymbol{d})$$

$$\approx \mathscr{T}_F([\boldsymbol{u}_h, p_h]) + \mathscr{T}_F([\tilde{\boldsymbol{u}}, 0]) + \mathscr{T}_S(\boldsymbol{d}_h) + \mathscr{T}_S(\tilde{\boldsymbol{d}}), \tag{47}$$

where $\tilde{\boldsymbol{d}}$ are the displacement subscales. Neglecting the subscales in the element interiors as before, $\mathscr{T}_F([\tilde{\boldsymbol{u}}, 0])$ can be approximated by $(\mu/\delta)\tilde{\gamma}_F$. The problem is how to approximate $\mathscr{T}_S(\tilde{\boldsymbol{d}})$. Approximating derivatives using finite differences will yield an expression of the form $\mathscr{T}_S(\tilde{\boldsymbol{d}}) \approx (1/\delta)\boldsymbol{G}\tilde{\gamma}_S$ for a certain matrix $\boldsymbol{G}$ depending on the physical parameters contained in the constitutive tensor $\boldsymbol{C}$. For our reasoning it is enough to approximate $\mathscr{T}_S(\tilde{\boldsymbol{d}}) \approx (G^*/\delta)\tilde{\gamma}_S$, G^* being a scalar coefficient. Altogether, (47) yields, on each edge of Γ,

$$G^* \tilde{\gamma}_S + \mu \tilde{\gamma}_F = -\delta[\mathscr{T}_F([\boldsymbol{u}_h, p_h]) + \mathscr{T}_S(\boldsymbol{d}_h)]. \tag{48}$$

The compatibility between the velocity in the fluid and the displacement in the solid implies also the compatibility in the corresponding subscales, that is to say, $\tilde{\gamma}_F = \partial_t \tilde{\gamma}_S$.

In FSI problems of interest, we may assume that the fluid and solid physical properties are such that

$$G^* |\tilde{\gamma}_S| \gg \mu |\partial_t \tilde{\gamma}_S|,$$

which using (48) implies that

$$\tilde{\gamma}_{\mathrm{S}} \approx -\frac{\delta}{G^*}[\mathscr{T}_{\mathrm{F}}([\boldsymbol{u}_h, p_h]) + \mathscr{T}_{\mathrm{S}}(\boldsymbol{d}_h)], \quad \tilde{\gamma}_{\mathrm{F}} \approx \boldsymbol{0},$$

and, consequently,

$$\boldsymbol{\lambda}_{\mathrm{S}} = \mathscr{T}_{\mathrm{S}}(\boldsymbol{d}_h) + \frac{G^*}{\delta}\tilde{\gamma}_{\mathrm{S}} \approx -\mathscr{T}_{\mathrm{F}}([\boldsymbol{u}_h, p_h]), \tag{49}$$

$$\boldsymbol{\lambda}_{\mathrm{F}} = \mathscr{T}_{\mathrm{F}}([\boldsymbol{u}_h, p_h]) + \tilde{\boldsymbol{\lambda}}_{\mathrm{F}} \approx \mathscr{T}_{\mathrm{F}}([\boldsymbol{u}_h, p_h]). \tag{50}$$

These approximations have an interesting consequence. Let $\boldsymbol{t}_{\mathrm{SF}} = -\boldsymbol{\lambda}_{\mathrm{F}} = -\mathscr{T}_{\mathrm{F}}([\boldsymbol{u}_h, p_h])$ be the stress *exerted on the solid* because of the interaction with the fluid, and $\boldsymbol{t}_{\mathrm{FS}} = -\boldsymbol{\lambda}_{\mathrm{S}} = \mathscr{T}_{\mathrm{F}}([\boldsymbol{u}_h, p_h])$ the stress *exerted on the fluid* because of the interaction with the solid. Suppose an iterative strategy is used to solve the fluid–solid coupling (within each time step, for example). If the solid is computed with a Neumann-type condition on Γ, $\boldsymbol{t}_{\mathrm{SF}} = -\mathscr{T}_{\mathrm{F}}([\boldsymbol{u}_h, p_h])$ has to be used as traction, which corresponds to the common approach: stresses computed in the fluid using the finite element solution are transmitted to the solid. In the fluid, a Dirichlet boundary condition on Γ can be used once the displacements in the solid have been computed. However, *it is not possible* to use a Neumann condition on Γ when solving in the fluid domain, since the traction to be used is $\boldsymbol{t}_{\mathrm{FS}} = \mathscr{T}_{\mathrm{F}}([\boldsymbol{u}_h, p_h])$, which depends only on the velocities. Thus, the fluid would not 'feel' the action exerted by the solid. This agrees with the well-known fact that in FSI problems if a Dirichlet–Neumann coupling is used, Neumann boundary conditions have to be applied always to the solid surface, not to the fluid.

A similar situation is encountered in homogeneous interaction problems if one of the subdomains is much 'stiffer' than the other. From (40) it is observed that if, for example, $\mu_1 \gg \mu_2$ then $\boldsymbol{\lambda}_1 = -\boldsymbol{\lambda}_2 \approx -\mathscr{T}_2([\boldsymbol{u}_h, p_h])$.

5.3. Fully discrete problem and iterative coupling

Suppose to simplify that time is discretized using a backward-difference formula, that we denote by D_t to approximate ∂_t and D_{tt} to approximate ∂_{tt}^2. Let δt be the time step size of a uniform partition of $[0, T]$. Consider that the unknowns are computed at time levels $0, 1, 2, ..., n-1$ and we want to compute them at time $t^n = n\delta t$. The fully discrete version of the problem corresponding to (39) is: find $\boldsymbol{d}_h^n \in W_h$, $\boldsymbol{u}_h^n \in V_h$ and $p_h^n \in Q_h$ such that

$$\rho_{\mathrm{S}}(D_{tt}\boldsymbol{d}_h^n, \boldsymbol{e}_h)_{\Omega_{\mathrm{S}}} + B_{\mathrm{S}}(\boldsymbol{d}_h^n, \boldsymbol{e}_h) - \frac{\delta}{G^*}\sum_{E_\Gamma}\langle \mathscr{T}_{\mathrm{S}}(\boldsymbol{d}_h^n), \mathscr{T}_{\mathrm{S}}(\boldsymbol{e}_h)\rangle_{E_\Gamma}$$

$$= L_{\mathrm{S}}(\boldsymbol{e}_h) + \langle \boldsymbol{t}_{\mathrm{SF}}, \boldsymbol{e}_h\rangle_\Gamma - \frac{\delta}{G^*}\sum_{E_\Gamma}\langle \boldsymbol{t}_{\mathrm{SF}}, \mathscr{T}_{\mathrm{S}}(\boldsymbol{e}_h)\rangle_{E_\Gamma}, \tag{51}$$

$$\rho_{\mathrm{F}}(D_t\boldsymbol{u}_h^n, \boldsymbol{v}_h)_{\Omega_{\mathrm{F}}} + B_{\mathrm{F,stab}}([\boldsymbol{u}_h^n, p_h^n], [\boldsymbol{v}_h, q_h]) - \frac{\delta}{\mu}\sum_{E_\Gamma}\langle \mathscr{T}_{\mathrm{F}}([\boldsymbol{u}_h^n, p_h^n]), \mathscr{T}_{\mathrm{F}}^*([\boldsymbol{v}_h, q_h])\rangle_{E_\Gamma}$$

$$= L_{\mathrm{F,stab}}([\boldsymbol{v}_h, q_h]) + \langle \boldsymbol{t}_{\mathrm{FS}}, \boldsymbol{v}_h\rangle_\Gamma - \frac{\delta}{\mu}\sum_{E_\Gamma}\langle \boldsymbol{t}_{\mathrm{FS}}, \mathscr{T}_{\mathrm{F}}^*([\boldsymbol{v}_h, q_h])\rangle_{E_\Gamma}, \tag{52}$$

which hold for all $\boldsymbol{e}_h \in W_h$, $[\boldsymbol{v}_h, q_h] \in V_h \times Q_h$. This is the *monolithic* fluid–structure system that we propose.

Of particular interest is the design of a simple iterative coupling between the solid and the fluid *using approximations* (49)–(50). Let us denote by $f^{n,i}$ an approximation to an unknown f at time step n and iteration i, with the initialization $f^{n,0} = f^{n-1}$. Suppose that the solid is solved first, with $[\boldsymbol{u}_h^{n,i-1}, p_h^{n,i-1}]$ known. Then, $\boldsymbol{t}_{\mathrm{SF}} = -\mathscr{T}_{\mathrm{F}}([\boldsymbol{u}_h^{n,i-1}, p_h^{n,i-1}])$ can be used in (51) to compute $\boldsymbol{d}_h^{n,i}$. When solving for the fluid, the traction to be used must be $\boldsymbol{t}_{\mathrm{FS}} = \mathscr{T}_{\mathrm{F}}([\boldsymbol{u}_h^{n,i-1}, p_h^{n,i-1}])$, since

only in this case one can guarantee that $t_{SF} + t_{FS} = 0$ *at each iteration.* Using this, and noting that $v_h|_\Gamma = 0$ if Dirichlet conditions are used to solve in the fluid domain, the algorithm reads

$$
\rho_S(D_{tt}d_h^{n,i}, e_h)_{\Omega_S} + B_S(d_h^{n,i}, e_h) - \frac{\delta}{G^*} \sum_{E_\Gamma} \langle \mathcal{T}_S(d_h^{n,i}), \mathcal{T}_S(e_h) \rangle_{E_\Gamma}
$$

$$
= L_S(e_h) - \langle \mathcal{T}_F([u_h^{n,i-1}, p_h^{n,i-1}]), e_h \rangle_\Gamma + \frac{\delta}{G^*} \sum_{E_\Gamma} \langle \mathcal{T}_F([u_h^{n,i-1}, p_h^{n,i-1}]), \mathcal{T}_S(e_h) \rangle_{E_\Gamma},
$$

$$
\rho_F(D_t u_h^{n,i}, v_h)_{\Omega_F} + B_{F,\text{stab}}([u_h^{n,i}, p_h^{n,i}], [v_h, q_h]) - \frac{\delta}{\mu} \sum_{E_\Gamma} \langle \mathcal{T}_F([u_h^{n,i}, p_h^{n,i}]), \mathcal{T}_F^*([v_h, q_h]) \rangle_{E_\Gamma}
$$

$$
= L_{F,\text{stab}}([v_h, q_h]) - \frac{\delta}{\mu} \sum_{E_\Gamma} \langle \mathcal{T}_F([u_h^{n,i-1}, p_h^{n,i-1}]), \mathcal{T}_F^*([v_h, q_h]) \rangle_{E_\Gamma}, \tag{53}
$$

with the essential condition $u_h^{n,i}|_\Gamma = D_t d_h^{n,i}|_\Gamma$ for the second equation. It is observed that:

- The second term on the RHS of the first equation enforces the continuity of tractions between the solid and the fluid when tested by the displacement test function.
- The third term on the LHS and the third term on the RHS of the first equation enforce further this continuity, now by testing the tractions with $\mathcal{T}_S(e_h)$. However, these terms are multiplied by δ/G^*, which is very small when realistic physical properties are used. Thus, their effect is in practice negligible.
- The crucial term is the second one on the RHS of the second equation. If it were evaluated at iteration i, it would cancel with the third term on the LHS, which would in fact lead to the simplest fluid–structure iterative algorithm. However, evaluating it at $i-1$ allows us to guarantee that $t_{SF} + t_{FS} = 0$ at each iteration, as it has been said, and also acts as a penalization of the jump of fluid tractions between iterations, given by $\mathcal{T}_F([u_h^{n,i}, p_h^{n,i}]) - \mathcal{T}_F([u_h^{n,i-1}, p_h^{n,i-1}])$. The bottom line of our formulation applied to FSI iterative algorithms can be summarized by these terms, which can *a posteriori* be understood as a modification of the simplest iterative scheme (more sophisticated algorithms could also be used). Numerical experiments show that the improvement in convergence observed well deserves their derivation.

6. NUMERICAL EXAMPLES

In this section, we present some numerical examples corresponding to the formulation presented in Sections 4 and 5. The ability of the method to use arbitrary discontinuous pressure interpolations for the pressure was already demonstrated in [6].

In all cases we will use the simplest choice $\tilde{P} = I$ in (38), where I is the identity (at least when applied to the residual of the finite element solution). This corresponds to the most popular stabilized finite element method for the Stokes problem. All the examples have been run using continuous P_1 elements (linear triangles in 2D) for all variables. The algorithmic constant C_1 in (33) has been set to $C_1 = 4$. When approximating the elasticity equations, $G^* = E$, Young's modulus, has been chosen in (51).

6.1. Two examples of domain interaction

In this subsection, we present the numerical results for two examples that illustrate the ideas presented in Section 4, one of a solid–solid interaction and another of a fluid–fluid interaction.
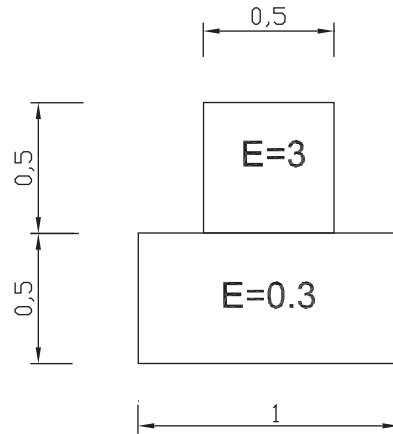
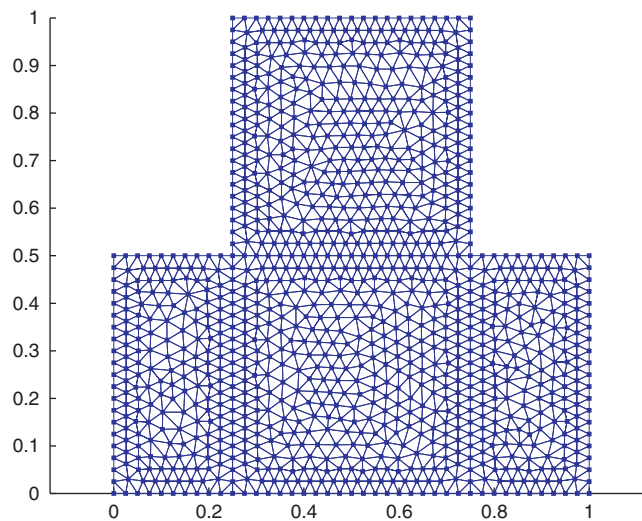Figure 4. Incompressible elastic bodies. Problem setting.

Figure 5. Incompressible elastic bodies. Finite element mesh.

The first example we consider consists of two incompressible elastic bodies, which we will model by means of the Stokes equations, now μ being the shear modulus. The problem setting and subdomains can be seen in Figure 4. Both bodies are incompressible (Poisson ratio $v=0.5$), but the body on the top is 10 times stiffer (Young's modulus $E=3$) than the one below (Young's modulus $E=0.3$). The unstructured triangular mesh consisting of 1990 triangles used to solve the problem can be seen in Figure 5.

The displacement and pressure fields obtained are shown in Figure 6. We also depict the normal tractions on the solid body interface, which coincide with the component σ_{22} of the stress tensor, in Figure 7. In can be observed that using subscales reduces the jump in tractions between both solid bodies, but the solution is stable and very similar whether subscales on the boundaries are used or not.

In the second example, we will consider the stationary cavity flow example for the Stokes problem. The fluid domain is given by $\Omega=[0,1]\times[0,1]$. All the boundaries are set to null velocity except for the one corresponding to $y=1$, in which we impose a horizontal velocity $u_x=1$ and a vertical velocity $u_y=0$. The fluid viscosity is set to $v=1$. A finite element mesh of 7200 structured triangles ($h=0.16$) has been used.
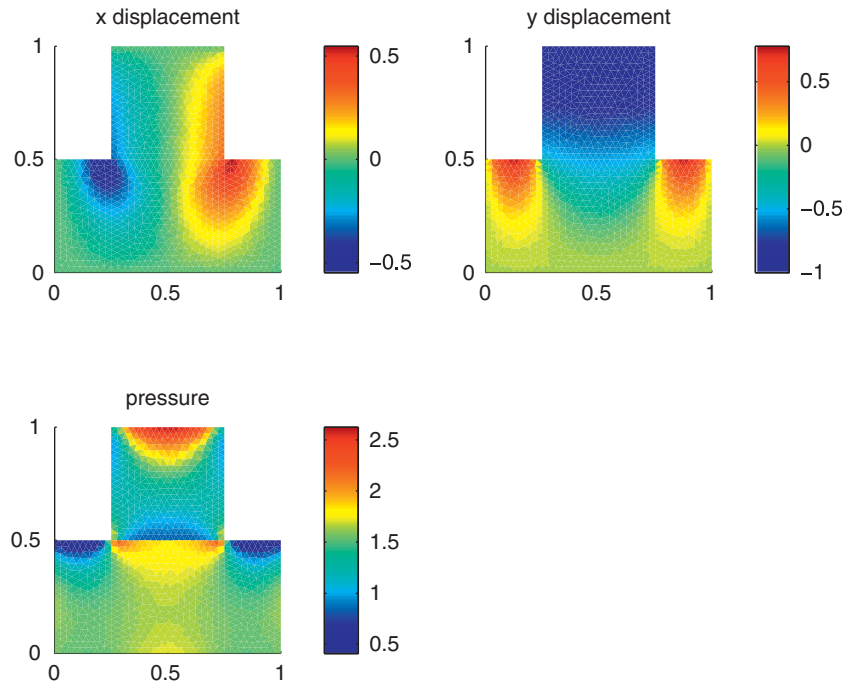
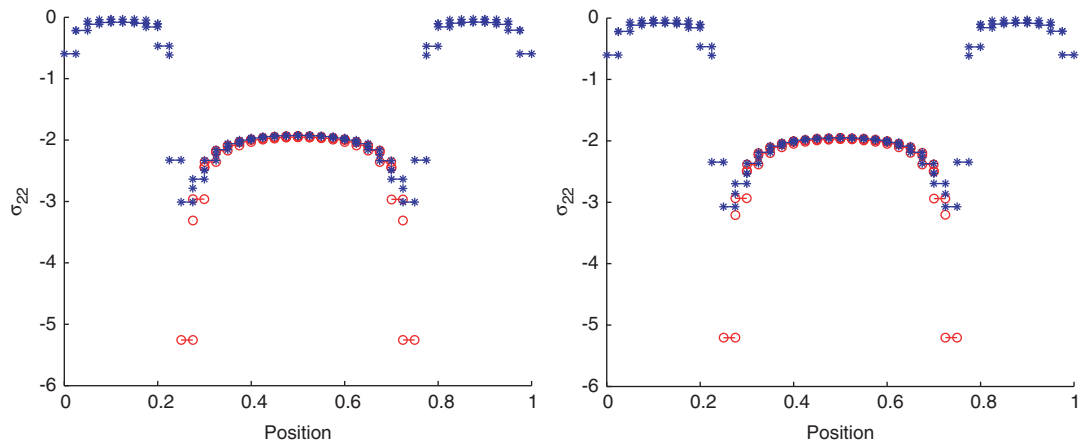Figure 6. Incompressible elastic bodies. Displacement and pressure fields.

Figure 7. Incompressible elastic bodies. Normal tractions along the interface for the upper (circles) and the lower (stars) solid bodies. Left: without subscales. Right: with subscales, $\delta_0 = 0.5$.

We now divide the fluid domain into two: the first subdomain corresponds to $x < 0.1$, whereas the second subdomain corresponds to $x > 0.1$. We solve this numerical example by means of a domain decomposition method and the GMRES strategy described in Section 4.5.

The velocity and pressure fields for the Stokes cavity problem are depicted in Figure 8. Since the fluid density and viscosity are the same in both subdomains, there should be no pressure jump in the boundary separating them. However, a pressure jump appears in the numerical solution which is due to the fact that extra pressure degrees of freedom have been added to the nodes belonging to the boundary. This pressure jump can be seen in Figure 9. We can see that using subscales on the element boundaries helps reduce the pressure jump, and as a consequence the pressure field gets closer to the one we would obtain if a monolithic approach was used, in which the pressure field would be continuous.
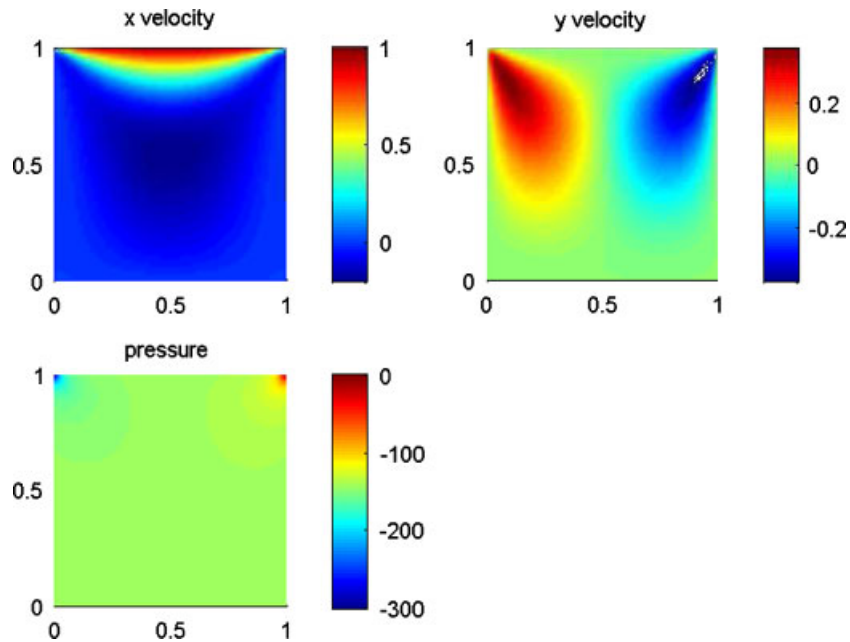
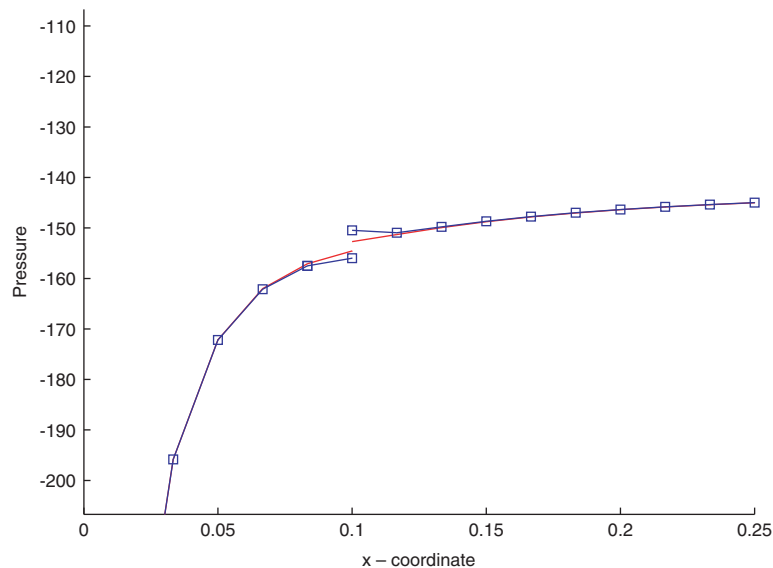Figure 8. Velocity and pressure fields for the Stokes cavity problem.

Figure 9. Pressure jump at $x = 0.1$. Squares: solution with subscales.

6.2. Added-mass effect

In this section, we present some numerical results that illustrate the behavior of the subscales on the element boundaries as strategy to alleviate the added-mass effect. In order to do so, we will use the example proposed in [10], in which we will couple the 2D Stokes equations with the linear elasticity equations.

The fluid domain is given by $\Omega_F = [0, 5] \times [0, 0.5]$ and the solid domain by $\Omega_S = [0, 5] \times [0.5, 0.6]$. Initially, both the fluid and the structure are at rest. The boundary conditions are as follows. In the structure domain, we impose null displacement at $x = 0$ and $x = 5$, while zero traction is applied on $y = 0.6$. For the fluid, we impose slip boundary conditions at $y = 0.0$, and an over-pressure of
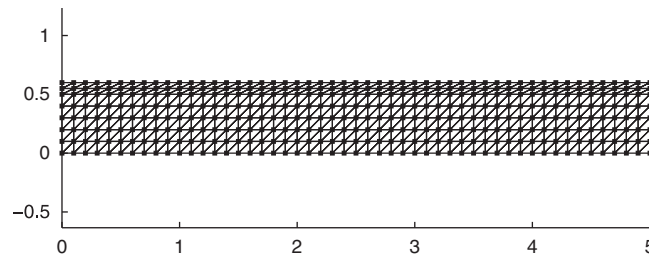
Figure 10. Finite element mesh.

10^4 during 5×10^{-3} time units. For the coupling between fluid and structure, we also impose slip boundary conditions, that is:

- Velocity continuity is imposed only in the direction normal to the fluid–structure interface.
- We impose traction continuity in the direction normal to the interface, but we do not consider tangent tractions.

The spatial discretization is carried out by means of a finite element mesh, its size being $h = 0.1$ (see Figure 10), and the time step is set to $\delta t = 10^{-4}$. The backward Euler scheme is used for the integration of the transient Stokes equations in the fluid, and the explicit second-order Newmark method is chosen for the time integration of the linear elasticity equations in the solid.

The main purpose of this numerical example is to compare the behavior of the numerical scheme with or without considering the contribution of the subscales on the element boundaries, and in particular regarding the added-mass effect.

We will first consider no subscales on the element boundaries and a Dirichlet–Neumann coupling strategy: we apply Dirichlet boundary conditions to the fluid domain and Neumann boundary conditions to the solid one. The iterative scheme we use is (53), considering the possibility to iterate within each time step to converge to the solution of the monolithic problem or without iterations. In this last case, corresponding to the so-called staggered schemes (or also 'loose coupling'), there is an error of the order of the time step size with respect to the solution of the monolithic problem. In (53), we will also consider the possibility of removing the terms coming from the subscales on the boundaries.

Initially, we consider a fluid density $\rho_F = 1.1$ and a viscosity $\mu = 0.035$. For the solid, we take a density $\rho_S = 1.2$, Young's modulus $E = 3 \times 10^8$ and the Poisson ratio $v = 0.0$. If we consider an explicit coupling (we do not iterate until convergence at each time step), the numerical scheme explodes, and we obtain an unstable numerical solution. We now consider a coupling strategy that involves convergence at each time step, in particular we impose that the relative error between the solution obtained at iteration i and iteration $i+1$ is less than 10^{-3}. Owing to the added-mass effect, this simple Dirichlet–Neumann scheme does not converge, and we need to use some additional tool in order to achieve the solution of the monolithic problem. Among the various existing methods, we can use a relaxation scheme. We have found it effective to take a relaxation parameter $\alpha = 0.3$ in (45). Figure 11 shows the vertical displacement at a solid point placed at the center of the solid domain. Figure 12 shows the velocity and pressure fluid fields at $t = 75 \times 10^{-4}$. The mean number of iterations at each time step was 26 for this numerical scheme.

Let us now consider the use of the subscales on the element boundaries, for which we will take $\delta_0 = 0.5 \times 10^{-3}$. If we try to use an explicit coupling scheme, the method fails again due to the added-mass effect, and we obtain an unstable solution. However, if we iterate at each time step and converge to the monolithic solution, we obtain the solution depicted in Figure 13, which is exactly equal to the one obtained without using subscales on the element boundaries, since the additional terms due to the use of these subscales vanish when convergence is achieved. However, we did not need to use relaxation in this case, and the mean number of iterations was substantially reduced to 5, with the subsequent reduction in the CPU time required to perform the computations.
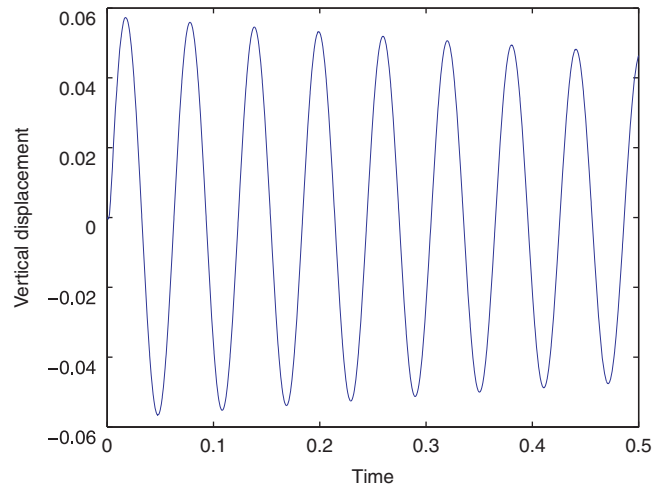
Figure 11. Results for the iterative scheme, no subscales, relaxation parameter $\alpha = 0.3$.
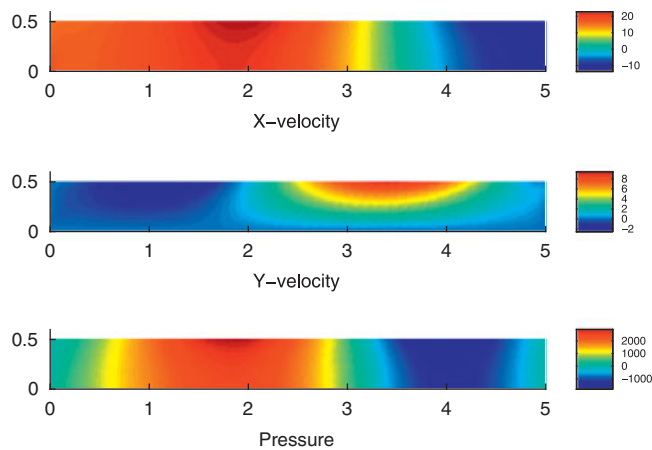

Figure 12. Velocity and pressure fluid fields at $t = 75 \times 10^{-4}$.

Let us now consider a less demanding situation, in which the solid density is $\rho_S = 20$. In this case, the ρ_S / ρ_F ratio is around 20 too. This means that the added-mass effect is not as severe as it was in the previous example, and that there might be no need to use an iterative scheme. We now test the explicit scheme with and without subscales on the element boundaries. In the first case, we take $\delta_0 = 1 \times 10^{-3}$. Figure 14 shows the results obtained with both schemes. We can see that the scheme becomes unstable after a few time steps if no subscales are used, but it remains stable, even for the explicit scheme, if the strategy we propose is used.

7. CONCLUSIONS

In this paper, we have motivated the introduction of element boundary terms in the finite element approximation the Stokes and the linear elasticity problems. The starting point has been the splitting of the unknowns of the problem into a conforming part and a discontinuous one, introducing a hybrid formulation only for the latter (Section 2). Although this approach could serve different purposes, in Section 3 we propose a finite element approximation in which the discontinuous component of the solution, its traces and fluxes are approximated by expressions that involve only the conforming part of the solution. The resulting formulation is a stabilized finite element method
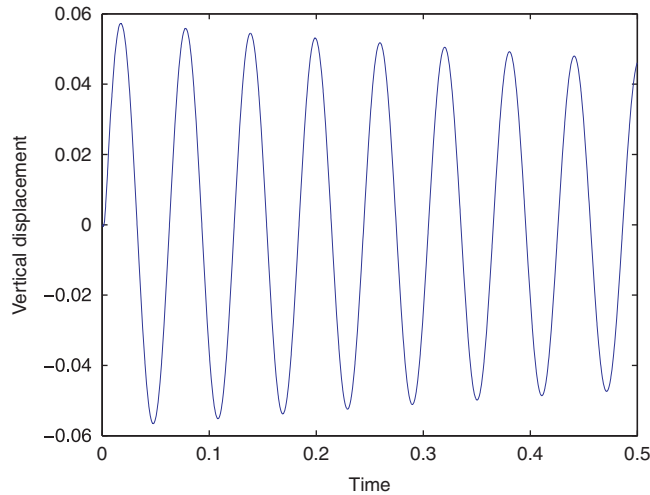
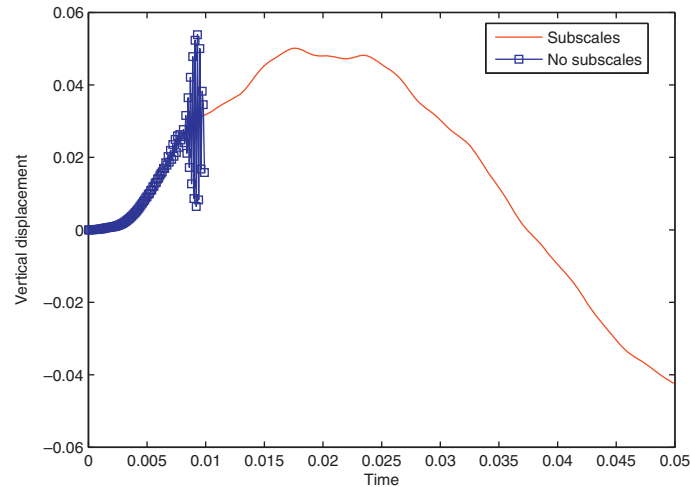Figure 13. Results for the iterative scheme with subscales, no relaxation.

Figure 14. Comparison between results with and without using subscales in the case of a ratio ρ_S/ρ_F around 20 and an explicit scheme.

for the Stokes problem that allows arbitrary interpolations of velocities and pressure. Particular emphasis has been given here on the treatment of Neumann-type boundary conditions.

The same ideas have been applied to the homogeneous interaction between two subdomains (Section 4). In this case, the benefit of the boundary terms is a stronger enforcement of the continuity of fluxes between subdomains. The matrix structure of the resulting system has been described and iterative schemes to be used in an iteration-by-subdomain environment have been proposed.

The FSI problem has then been treated (Section 5). The extension of the previous ideas to this case has led to a modification of what can be considered a classical solid–fluid iterative coupling. The boundary terms introduced, which cancel when convergence is achieved, would hardly be motivated from a purely algebraic point of view.

All our predictions have been stated based on physical reasoning, without numerical analysis (although we have done this analysis in what concerns the stability and convergence of the method when applied to a single domain, showing that indeed arbitrary velocity–pressure interpolations can be used, see [6]). Numerical experiments have confirmed the theoretical predictions. In particular,

a better enforcement of the continuity of fluxes is found in homogeneous domain interaction problems and, what is probably the most salient result of this work, convergence of solid–fluid iterative coupling algorithms is greatly improved by the terms we suggest to introduce.

REFERENCES

1. Quarteroni A, Valli A. *Domain Decomposition Methods for Partial Differential Equations*. Oxford Science Publications: Oxford, 1999.
2. Toselli A, Windlun O. *Domain Decomposition Methods—Algorithms and Theory*. Springer: Berlin, 2005.
3. Hughes TJR, Feijóo GR, Mazzei L, Quincy JB. The variational multiscale method—a paradigm for computational mechanics. *Computer Methods in Applied Mechanics and Engineering* 1998; **166**:3–24.
4. Brezzi F, Fortin M. *Mixed and Hybrid Finite Element Methods*. Springer: Berlin, 1991.
5. Hughes TJR, Franca LP, Hulbert GM. A new finite element formulation for computational fluid dynamics: VII. The Stokes problem with various well-posed boundary conditions: symmetric formulations that converge for all velocity/pressure spaces. *Computer Methods in Applied Mechanics and Engineering* 1987; **65**:85–96.
6. Codina R, Principe J, Baiges J. Subscales on the element boundaries in the variational two-scale finite element method. *Computer Methods in Applied Mechanics and Engineering* 2009; **198**:838–852.
7. Fernandez MA, Gerbeau J-F, Grandmont C. A projection semi-implicit scheme for the coupling of an elastic structure with an incompressible fluid. *International Journal for Numerical Methods in Engineering* 2007; **69**:794–821.
8. Astorino M, Chouly F, Fernandez MA. An added-mass free semi-implicit coupling scheme for fluid–structure interaction. *Comptes Rendus de l'Académie des Sciences, Série I* 2009; **347**:99–104.
9. Idelsohn SR, Del Pin F, Rossi R, Oñate E. Fluid–structure interaction problems with strong added-mass effect fluid incompressibility. *International Journal for Numerical Methods in Engineering* 2009; **80**:1261–1294.
10. Burman E, Fernandez MA. Stabilization of explicit coupling in fluid–structure interaction involving fluid incompressibility. *Computer Methods in Applied Mechanics and Engineering* 2009; **198**:766–784.
11. Badia S, Nobile F, Vergara C. Fluid–structure partitioned procedures based on Robin transmission conditions. *Journal of Computational Physics* 2008; **227**:7027–7051.
12. Badia S, Nobile F, Vergara C. Robin–Robin preconditioned Krylov methods for fluid–structure interaction problems. *Computer Methods in Applied Mechanics and Engineering* 2009; **198**:2768–2784.
13. Badia S, Quaini A, Quarteroni A. Modular vs non-modular preconditioners for fluid–structure systems with large added-mass effect. *Computer Methods in Applied Mechanics and Engineering* 2008; **197**:4216–4232.
14. Badia S, Quaini A, Quarteroni A. Splitting methods based on algebraic factorization for fluid–structure interaction. *SIAM Journal on Scientific Computing* 2008; **30I4**:1778–1805.
15. Forster C, Wall WA, Ramm E. Artificial added mass instabilities in sequential staggered coupling of nonlinear structures and incompressible viscous flows. *Computer Methods in Applied Mechanics and Engineering* 2007; **196**:1278–1293.
16. Cockburn B, Gopalakrishnan J, Lazarov R. Unified hybridization of discontinuous Galerkin, mixed, and continuous Galerkin methods for second order elliptic problems. *SIAM Journal on Numerical Analysis* 2009; **47**:1319–1365.
17. Cockburn B, Dong B, Guzman J, Restelli M, Sacco R. A hybridizable discontinuous Galerkin method for steady-state convection–diffusion-reaction problems. *SIAM Journal on Scientific Computing* 2009; **31**:3827–3846.
18. Nguyen NC, Peraire J, Cockburn B. An implicit high-order hybridizable discontinuous Galerkin method for linear convection–diffusion equations. *Journal of Computational Physics* 2009; **228**:3232–3254.
19. Rapin G, Lube G. A stabilized three-field formulation for advection-diffusion equations. *Computing* 2004; **73**:155–178.
20. Codina R. Stabilized finite element approximation of transient incompressible flows using orthogonal subscales. *Computer Methods in Applied Mechanics and Engineering* 2002; **191**:4295–4321.
21. Codina R. Analysis of a stabilized finite element approximation of the Oseen equations using orthogonal subscales. *Applied Numerical Mathematics* 2008; **58**:264–283.
22. Houzeaux G, Codina R. A Chimera method based on a Dirichlet/Neumann (Robin) coupling for the Navier–Stokes equations. *Computer Methods in Applied Mechanics and Engineering* 2003; **192**:3343–3377.
23. Codina R, Houzeaux G, Coppola-Owen H, Baiges J. The fixed-mesh ALE approach for the numerical approximation of flows in moving domains. *Journal of Computational Physics* 2009; **228**:1591–1611.
24. Houzeaux G, Codina R. Transmission conditions with constraints in finite element domain decomposition methods for flow problems. *Communications in Numerical Methods in Engineering* 2001; **17**:179–190.